THE UNIVERSITY OF MICHIGAN

COLLEGE OF ENGINEERING
High Altitude Engineering Laboratory
Department of Aerospace Engineering
Department of Meteorology and Oceanography

Quarterly Report

HIGH ALTITUDE RADIATION MEASUREMENTS

1 January 1969 - 31 March 1969

Fred L. Bartman

ORA Project 05863

under contract with:

NATIONAL AERONAUTICS AND SPACE ADMINISTRATION
CONTRACT NO. NASr-54(03)
WASHINGTON, D. C.

administered through:

OFFICE OF RESEARCH ADMINISTRATION ANN ARBOR

May 1969

Table of Contents

List of Tables

List of Illustrations

Abstract

This report summarizes project activity during the period 1 January to 30 March 1969. Topics discussed are:

1. Analysis and processing of data for 20 November 1968 balloon flight.
2. Medium and high resolution measurements of the 15 μm absorption band of CO_2.
3. Determination of the vertical distribution of O_3 from radiance measurements in the 9.6 μm band.
4. Laboratory tests of the IRIS interferometer.
5. Study of techniques for measuring molecular collision rates.
6. Microwave occultation studies

I. Introduction

This is the 25th Quarterly Progress Report on Contract No. NASr-54(03) covering the period 1 January to 31 March, 1969. The project effort during this period of time was divided among the following tasks.

1. Analysis and processing of data for 20 November 1968 balloon flight.
2. Medium and high resolution measurements of the 15 μm absorption band of CO_2.
3. Determination of the vertical distribution of O_3 from radiance measurements in the 9.6 μm band.
4. Laboratory tests of the IRIS interferometer.
5. The study of techniques for measuring molecular collision rates.
6. Microwave occultation studies.
7. Report writing.

II. Analysis and Processing of Data for 20 November 1968 Balloon Flight

Some of the basic data on the balloon flight were reported on in the last quarterly report 05863-24-P. Figures 20-27 of that report include data on the balloon configuration, the balloon trajectory, a temperature vs. altitude curve, and housekeeping data on the Filter Wedge Spectrometer, the MRIR radiometer and the balloon gondola. Some of that data is included in this report for completeness. Thus this report will contain a complete set of data on the balloon flight for data analysis purposes.

A. Balloon Trajectory

The balloon configuration is shown in figure 1 and characteristics of the balloon flight trajectory are shown in figures 2 and 3. Figure 2 shows pressure altitude versus time and also shows the temperature versus altitude data taken by the radiosonde unit carried on the balloon gondola. Figure 3 shows the ground trace of the balloon trajectory. A photo of the balloon as viewed from the balloon gondola just before cutdown is shown in figure 4. Figure 5 shows the parachute as viewed from the balloon gondola during descent.

B. Aerial Photography

Table I describes the aerial photographs obtained on balloon flight 11. The time at which each photograph was taken by cameras 1 and 2 is given in table II. Table III gives the time for each photograph taken by camera 3.

TABLE I

Aerial Photographs Available for Balloon Flight II

Camera No.	Film Type	Field of View Sides	Field of View Corners	Direction of View	Number of Photos	Time Interval of Photos
1	IR Ektachrome	41.6°	56.5°	Downward	357	0949:29-1611 EST
2	Plus X	21.5°	30.1°	Downward	415	0849:46-1611 EST
3	Plus X	73.7°	93.4°	Sideward	166	0849:46-1611 EST
4	Ektachrome EF	73.7°	93.4°	Sideward	---*	----------

*Focal plane shutter inoperative.

TABLE II

TIME[1] FOR EACH PHOTOGRAPH TAKEN BY CAMERAS #1 AND #2

Photo #	Est.	Photo #	Est.	Photo #	Est.	Photo #	Est.	Photo #	Est.	Photo #	Est.	Photo #	Est.	Photo #	Est.	Photo #	Est.
Camera #3 & #4 start → 2	0849:46	51	0942:01	100	1034:16	149	1126:30	198	1218:47	247	1311:04	296	1403:18	345	1455:37	394	1547:52
3	0850:50	52	0943:05	101	1035:20	150	1127:34	199	1219:51	248	1312:08	297	1404:22	346	1456:41	395	1548:56
4	0851:54	53	0944:09	102	1036:24	151	1128:38	200	1220:55	249	1313:12	298	1405:26	347	1457:45	396	1550:00
5	0852:58	54	0945:13	103	1037:28	152	1129:42	201	1221:58	250	1314:16	299	1406:30	348	1458:49	397	1551:04
6	[0854:02]	55	0946:17	104	1038:32	153	1130:50	202	1223:02	251	1315:20	300	1407:34	349	1459:53	398	-- [5]
7	0855:06	56	0947:21	105	1039:36	154	1131:54	203	1224:06	252	1316:24	301	1408:38	350	1500:57	.	
8	0856:10	57	0948:25	106	1040:40	155	1132:58	204	1225:10	253	1317:28	302	1409:42	351	1502:01	.	
9	0857:14	Camera #1 start → 58	0949:29	107	1041:44	156	1134:02	205	1226:14	254	1318:32	303	1410:48	352	1503:05	.	
10	0858:18	59	0950:33	108	1042:48	157	1135:06	206	1227:18	255	1319:36	304	1411:52	353	1504:08	415	--
11	0859:22	60	0951:37	109	1043:52	158	1136:10	207	1228:22	256	1320:40	305	1412:56	354	1505:12		
12	0900:26	61	0952:41	110	1044:56	159	1137:14	208	1229:26	257	1321:44	306	1414:00	355	1506:16		
13	0901:30	62	0953:45	111	1046:00	160	1138:18	209	1230:30	258	1322:48	307	1415:04	356	1507:20		
14	[0902:34]	63	0954:49	112	1047:04	161	1139:22	210	1231:36	259	1323:52	308	1416:08	357	1508:24		
15	0903:38	64	0955:53	113	1048:07	162	1140:26	211	1232:40	260	1324:56	309	1417:12	358	1509:28		
16	0904:42	65	0956:57	114	1049:11	163	1141:30	212	1233:44	261	1326:00	310	1418:16	359	1510:32		
17	0905:46	66	0958:01	115	1050:15	164	1142:34	213	1234:48	262	1327:04	311	1419:20	360	1511:36		
18	0906:50	67	0959:05	116	1051:19	165	1143:36	214	1235:52	263	1328:08	312	1420:24	361	1512:40		
19	0907:54	68	1000:09	117	1052:23	166	1144:40	215	1236:56	264	1329:12	313	1421:28	362	1513:44		
20	0908:58	69	1001:13	118	1053:27	167	1145:44	216	1238:00	265	1330:16	314	1422:32	363	1514:48		
21	0910:02	70	1002:17	119	1054:31	168	1146:48	217	1239:04	266	1331:20	315	1423:36	364	1515:52		
22	0911:06	71	1003:21	120	1055:35	169	1147:52	218	1240:08	267	1332:24	316	1424:40	365	1516:56		
23	0912:10	72	1004:25	121	1056:38	170	1148:56	219	1241:12	268	1333:28	317	1425:44	366	1518:00		
24	0913:14	73	1005:29	122	1057:42	171	1150:00	220	1242:16	269	1334:31	318	1426:48	367	1519:04		
25	0914:18	74	1006:33	123	1058:46	172	1151:04	221	1243:20	270	1335:35	319	1427:52	368	1520:08		
26	0915:22	75	1007:37	124	1059:50	173	1152:07	222	1244:24	271	1336:39	320	1428:56	369	1521:12		
27	0916:26	76	1008:41	125	1100:54	174	1153:11	223	1245:28	272	1337:43	321	1430:00	370	1522:16		
28	0917:30	77	1009:45	126	1101:58	175	1154:15	224	1246:32	273	1338:47	322	1431:04	371	1523:20		
29	0918:34	78	1010:49	127	1103:02	176	1155:19	225	1247:36	274	1339:51	323	1432:08	372	1524:24		
30	0919:38	79	1011:53	128	1104:06	177	1156:23	226	1248:40	275	1340:55	324	1433:12	373	1525:28		
31	0920:42	80	1012:57	129	1105:09	178	1157:27	227	1249:44	276	1341:59	325	1434:15	374	1526:32		
32	0921:46	81	1014:01	130	1106:13	179	1158:31	228	1250:48	277	1343:03	326	1435:19	375	1527:36		
33	0922:50	82	1015:05	131	1107:17	180	1159:35	229	1251:52	278	1344:07	327	1436:23	376	1528:40		
34	0923:54	83	1016:09	132	1108:21	181	1200:39	230	1252:56	279	1345:11	328	1437:27	377	1529:44		
35	0924:58	84	1017:13	133	1109:24	182	1201:43	231	1254:00	280	1346:15	329	1438:31	378	1530:48		
36	0926:02	85	1018:17	134	1110:28	183	1202:47	232	1255:04	281	1347:19	330	1439:35	379[4]	1531:52		
37	0927:06	86	1019:21	135	1111:32	184	1203:51	233	1256:08	282	1348:23	331	1440:39	380	1532:56		
38	0928:10	87	1020:25	136	1112:36	185	1204:55	234	1257:12	283	1349:27	332	1441:43	381	1534:00		
39	0929:14	88	1021:29	137	1113:40	186	1205:59	235	1258:16	284	[1350:31]	333	1442:46	382	1535:04		
40	0930:18	89	1022:33	138	1114:44	187	1207:03	236	1259:20	285	[1351:35]	334	1443:50	383	1536:08		
41	0931:22	90	1023:37	139	1115:48	188	1208:07	237	1300:24	286	[1352:39]	335	1444:54	384	1537:12		
42	0932:26	91	1024:41	140	1116:52	189	1209:11	238	1301:28	287	[1353:43]	336	1445:58	385	1538:16		
43	0933:30	92	1025:45	141	1117:56	190	1210:15	239	1302:32	288	1354:47	337	1447:05	386	1539:20		
44	0934:34	93	1026:48	142	1119:00	191	1211:19	240	1303:36	289	1355:51	338	1448:09	387	1540:24		
45	0935:37	94	1027:52	143	1120:07	192	1212:23	241	1304:40	290	1356:55	339	1449:13	388	1541:28		
46	0936:41	95	1028:56	144	1121:11	193	1213:27	242	1305:44	291	1357:59	340	1450:17	389	1542:32		
47	0937:45	96	1030:00	145	1122:15	194	1214:31	243	1306:48	292	1359:03	341	1451:21	390	1543:36		
48	0938:49	97	1031:04	146	1123:19	195	1215:35	244	1307:52	293	1400:06	342	1452:25	391	1544:40		
49	0939:53	98	1032:08	147	1124:23	196	1216:39	245	1308:56	294	1401:10	343	1453:29	392	1545:44		
50	0940:57	99	1033:12	148	1125:27	197	1217:43	246	1310:00	295	1402:14	344	1454:33	393	1546:48		

NOTE

1. All photos taken about 0.3 sec before time indicated.
2. [ ] indicates time estimated, telemetry record missing.
3. ___ _____ indicates shift in time between gondola programmer clock and E. S. T.
4. Gondola cut down at 1531 E. S. T.
5. Telemetry signal no longer received, therefore exact photo times not available. Add 1 min and 4 sec. for each photo after #397.

TABLE III

Time For Each Photograph Taken by Camera #3

Photo#	EST	Photo#	EST	Photo#	EST	Photo#	EST	Photo#	EST	Photo#	EST
1	0849:46	31	1009:45	61	1129:42	91	1249:44	121	1409:42	151	1529:44
2	0851:54	32	1011:53	62	1131:54	92	1251:52	122	1411:52	152	1531:52
3	0855:06	33	1015:15	63	1135:06	93	1255:04	123	1415:04	153	1535:04
4	0857:14	34	1017:13	64	1137:14	94	1257:12	124	1417:12	154	1537:12
5	0900:26	35	1020:25	65	1140:26	95	1300:24	125	1420:24	155	1540:24
6	0902:34	36	1022:33	66	1142:34	96	1302:32	126	1422:32	156	1542:32
7	0905:46	37	1025:45	67	1145:44	97	1305:44	127	1425:44	157	1545:44
8	0907:54	38	1027:52	68	1147:52	98	1307:52	128	1427:52	158	1547:52
9	0911:06	39	1031:04	69	1151:04	99	1311:04	129	1431:04	159	1551:04
10	0913:14	40	1033:12	70	1153:11	100	1313:12	130	1433:12	160	
11	0916:26	41	1036:24	71	1156:23	101	1316:24	131	1436:23	161	
12	0918:34	42	1038:32	72	1158:31	102	1318:32	132	1438:31	162	
13	0921:46	43	1041:44	73	1201:43	103	1321:44	133	1441:43	163	
14	0923:54	44	1043:52	74	1203:51	104	1323:52	134	1443:50	164	
15	0927:06	45	1047:04	75	1207:03	105	1327:04	135	1447:05	165	
16	0924:14	46	1049:11	76	1209:11	106	1329:12	136	1449:13	166	
17	0932:26	47	1052:23	77	1212:23	107	1332:24	137	1452:25		
18	0934:34	48	1054:31	78	1214:31	108	1334:31	138	1454:33		
19	0937:45	49	1057:42	79	1217:43	109	1337:43	139	1457:45		
20	0939:53	50	1059:50	80	1219:51	110	1339:51	140	1459:53		
21	0943:05	51	1103:02	81	1223:02	111	1343:03	141	1503:05		
22	0945:13	52	1105:09	82	1225:10	112	1345:11	142	1505:12		
23	0948:25	53	1108:21	83	1228:22	113	1348:23	143	1508:24		
24	0950:33	54	1110:28	84	1230:30	114	1350:31	144	1510:32		
25	0953:45	55	1113:40	85	1233:44	115	1353:43	145	1513:44		
26	0955:53	56	1115:48	86	1235:52	116	1355:51	146	1515:52		
27	0959:05	57	1119:00	87	1239:04	117	1359:03	147	1519:04		
28	1001:13	58	1121:11	88	1241:12	118	1401:10	148	1521:12		
29	1004:25	59	1124:23	89	1244:24	119	1404:22	149	1524:24		
30	1006:33	60	1126:30	90	1246:32	120	1406:30	150	1526:32		

Figures 6, 7 and 8 are examples of photos taken by cameras 1, 2 and 3 respectively.

Figure 6 shows photograph 190 taken by camera #1 at 1210:15 EST. This camera has a 41.6° side to side field of view. Since the balloon was at 110,000 feet altitude, the photo shows an area on the surface which is 15.9 miles square. This photo was taken with IR etachrome film. The color rendition of this film for three representative botanical subjects is as follows:

Subject	Color
Healthy-deciduous, green foliage	Red
Diseased or deficient foliage	Greenish, bluish
Conifers	Dark purple

The color rendition of figure 3 may not be a faithful representation of the original, however it can be noticed that most of the photo is predominantly bluish in color, indicating that the surface is barren, i.e., the vegetation is mostly dead at this time of the year. The very dark purple area probably indicates the presence of conifers. All of the infrared photos taken have the characteristic greenish, bluish color indicative of barren surface. Occasionally in these photos some field will show a reddish tinge indicative of deciduous green foliage.

Figure 7 shows photograph 190 taken with camera #2, at the same time as photo 190 of camera #1 shown in figure 6. Camera #2 has 21.5° side to side field of view and therefore shows an almost square area on the surface about 8 miles wide. (The area is not precisely square, since it is the intersection of the square field of view with the spherical earth). Unfortunately, the focal plane shutter on this camera did not operate properly. Light was allowed to leak in on one side of each photo. As much as 30% of each photo is washed out because of this effect.

Figure 8 shows photo 75 taken with camera #3, at 1207:03 EST. This camera viewed the earth with its optical axis tilted at 45° to the vertical. Thus with its side to side field of view of 73.7° it views an area off to one side of the sub-balloon point, which in the vertical plane through the optical axis extends from 3.0 to 159.4 miles from the sub-balloon point.

C. Supporting Atmospheric Structure Data

1. Temperature and Relative Humidity Data from Conventional Radiosondes.

A considerable amount of temperature and relative humidity data were obtained from conventional radiosonde flights. Additional data was obtained on the ozonesonde flights which use a modified radiosonde unit. Temperature and relative humidity data obtained at Rapid City, S. D. are shown in figures 9-15; for Denver, Colo., figures 16-18; for Boulder, Colo. (Temperature and Ozone) figure 19; for N. Platte, Nebr., figures 20-24; for Bismarck, N. D., figures 25-28; and for Lander Wyo., figures 29-31.

Since the balloon trajectory was southward from Rapid City to Kimball, Nebraska, it seems that the temperature data obtained at Rapid City, Denver and Boulder, Color. and North Platte, Nebr. are most appropriate for determining atmospheric parameters for the balloon flight, therefore the temperature data for these locations has been listed in tables IV, V and IV. The rather significant temperature differences between the three locations, and time variations in temperature at Rapid City should be noticed when using this data for correlation with radiation data.

2. Special Frost Point Hygrometer Flights.

Two special radiosondes were flown at Rapid City by H. J. Mastenbrook of the Naval Research Laboratories to provide frost point hygrometer data to high altitudes. The data from these 2 flights is given in tables VII, VIII and IX. Mr. Mastenbrook's comments on the flights and on the data obtained are given below.

"Enclosed are the data tabulations for the two water vapor soundings at Rapid City on November 20. As you know, our flight configuration is designed to collect data during a balloon descent to avoid contamination from sources external to the sensing cavity. The ascent sounding is subject to large contamination error in the stratosphere, however, at lower tropospheric levels the contamination component is generally negligible. The tabulations therefore include the ascent data for the lower troposphere to the elevation where the ascent and descent data begin to diverge. Descent data is presented as far down as data was obtained.

A failure of the turn-around control on the first flight resulted in a fast parachute descent which did not yield reliable data. The flight did provide useable data for the lower tropospheric ascent.

TABLE IV

Temperature vs. Altitude Data, Rapid City, S. D.

Pressure Altitude mb	19 Nov. 2315Z	20 Nov. 1115Z	20 Nov. 1308Z	20 Nov. 1515Z	20 Nov. 2005Z	20 Nov. 2332Z	21 Nov 1733Z
900	2.8°C	9.8°C	2.5°C	--	17.5°C	13.2°C	
800	0	5.5	5.5	6.0	10.1	11.6	4.5
700	-1.0	0	0	2.8	4.0	9.7	-6.8
600	-8.7	-5.1	-4.2	-3.0	-1.5	-0.9	-10.2
500	-18.1	-14.0	-14.1	-11.0	-12.0	-13.1	-17.1
400	-29.0	-24.0	-24.0	-25.0	-25.0	-25.1	-27.3
300	-45.0	-42.0	-41.0	-40.0	-41.5	-41.5	-43.8
200	-60.0	-63.5	-61.0		-51.5	-59.0	-56.7
150	-56.1	-62.1	-62.5		-65.0	-66.0	-59.2
100	-60.5	-64.1	-64.5		-64.5	-67.5	-64.6
90	-61.4	-63.7	-63.9		-65.1	-65.8	-66.2
80	-62.4	-63.2	-63.3		-65.5	-64.0	-59.1
70	-61.5	-62.7	-62.7		-62.5	-62.0	-58.1
60	-60.0	-62.0	-62.1		-59.5	-59.9	-56.9
50	-59.6	-61.3	-61.3		-59.2	-59.8	-55.6
40	-60.8	-60.4	-60.5		-58.5	-59.1	-56.2
30	-59.3	-59.5	-59.3		-56.7	-56.0	-53.5
20		-58.3	-58.1			-56.0	-55.1
15		-57.5	-57.5			-59.0	-55.9
10							-54.9
9							-52.5
8							-49.9

TABLE V

Temperature vs. Altitude Data, Denver and Boulder, Colorado

Pressure Altitude mb	Denver 19 Nov. 2315Z	Denver 20 Nov. 1115Z	Boulder 20 Nov. 2043Z	Denver 20 Nov. 2315Z
900				
800	5.5°C	12.8°C	13.0°C	13.2°C
700	0.9	5.6	5.5	4.2
600	-8.0	-3.7	-3.5	-4.5
500	-16.6	-14.3	-10.5	-11.4
400	-28.6	-26.3	-23.5	-23.6
300	-45.3	-42.8	-40.7	-41.0
200	-59.0	-61.5	-58.0	-57.0
150	-56.4	-65.9	-63.0	-64.5
100	-62.1	-65.9	-67.2	-69.2
90	-64.6	-67.6	-66.5	-67.4
80	-66.5	-66.1	-65.3	-65.7
70	-63.9	-67.6	-64.5	-66.9
60	-62.4	-65.4	-63.2	-64.2
50	-63.9	-62.7	-61.5	-62.2
40	-59.9	-61.9	-59.5	-62.7
30	-62.1	-61.6	-57.1	-59.1
20	-59.6	-61.0	-53.5	-59.1
15			-55.1	
10			-50.9	
9				
8				

Table VI

Temperature vs. Altitude Data, North Platte, Nebraska

Pressure Altitude mb	19 Nov. 2315Z	20 Nov. 1115Z	20 Nov. 1723Z	20 Nov. 2315Z	21 Nov 1549Z
900	1.5°C		5.3°C	13.6°C	6.9°
800	-4.2	4.5°C	6.6	7.5	10.1
700	-5.6	0.8	4.0	4.1	2.1
600	-10.0	-5.6	-4.4	-2.6	-3.6
500	-19.0	-15.0	-10.3	-12.2	-13.4
400	-32.0	-25.0	-22.6	-25.2	-25.5
300	-46.8	-34.5	-38.6	-41.2	-41.9
200	-54.0	-63.2	-61.4	-62.5	-57.6
150	-54.5	-61.4	-63.5	-65.0	-63.2
100	-60.6	-63.5	-63.2	-65.0	-66.8
90	-62.2	-63.4	-62.5	-65.2	-65.9
80	-63.9	-63.3	-61.7	-65.5	-64.9
70	-63.9	-63.1	-60.8	-65.8	-63.8
60	-61.0	-63.0	-59.8	-64.7	-62.5
50	-60.9	-62.8	-58.5	-63.3	-61.0
40	-60.8	-61.8	-60.2	-61.7	-59.2
30	-60.5	-60.4	-57.7	-56.6	
20	-60.3	-58.3	-53.7	-60.4	
15	-57.8		-50.6	-58.4	
10	-52.3		-50.6	-53.5	
9			-50.8		
8			-51.0		
7			-49.0		

The three soundings through the troposphere indicate that atmospheric saturation was encountered in the general altitude range of 350 millibars to 400 or 450 millibars. The disturbed appearance of the ascent record above 350 millibars suggests that ice crystals were encountered. The apparent supersaturation observed in the interval is a further indication of an intake of ice crystal, since the sampled area in the sensing cavity is heated somewhat above ambient and can take on additional moisture through evaporation. Further evidence of saturation may appear in the sky photographs although a uniform thin cirrus may lack sufficient contrast to be identified on film.

The stratospheric distribution at Rapid City is in reasonable agreement with the distributions observed at Washington, D. C. in October and November, preceding and following the Rapid City flights. Please let us know if you have further questions about the data."

3. Ozone Data

Ozonesonde data for the unit launch at Boulder, Colo., by W. Komyhr and his colleagues is the only ozone data available for this flight. The ozone distribution obtained is shown in figure 19.

4. Atmospheric Parameter Support Data Obtained by Colorado State University

Personnel of Colorado State University flew their Aero-Commander 500B under the balloon during the flight and obtained data with the following apparatus:

a. A particle sampling system consisting of an air intake system and a Bausch and Lomb dust counter.

b. A Barnes IT-3 infrared radiometer looking vertically downward at the earth's surface.

c. An environmental temperature measuring system consisting of wet and dry bulb outside air temperature measurements.

The data obtained for this balloon flight is summarized in a report "Aero Commander 500B Support Data for Balloon Flight, November 20, 1968." by D. Adam, G. Cobb and B. Meline, Department of Atmospheric Science, Colorado State University, Fort Collins, Colorado, February 18, 1969.

TABLE VII

Frost Point Hygrometer Data Rapid City, South Dakota 11/20/68 1515Z Ascent

P(mb)	T(°C)	F(°C)	w(g/kg)	θ(°K)	M(cm)	∑M(cm)
867.00	9.2	-5.9	2.68298	294.1		
847.00	8.5	-5.9	2.74661	295.3	.05540381	.05540381
829.00	7.6	-5.3	2.94289	296.2	.05234218	.10774599
816.00	7.0	-5.3	3.00016	296.9	.03948437	.14723036
800.00	6.0	-5.9	2.90873	297.5	.04823567	.19546603
787.00	5.3	-6.4	2.81995	298.2	.03799623	.23346226
770.00	4.7	-7.5	2.61759	299.4	.04716215	.28062440
759.00	4.4	-8.0	2.53866	300.4	.02893798	.30956239
748.00	4.3	-9.1	2.35667	301.5	.02747369	.33703607
735.00	4.2	-9.6	2.29458	302.8	.03085001	.36788608
722.00	3.9	-8.6	2.54970	304.1	.03213026	.40001634
710.00	3.3	-8.6	2.59297	304.9	.03148557	.43150191
700.00	2.8	-8.6	2.63017	305.5	.02664855	.45815046
686.00	1.9	-8.6	2.68408	306.4	.03795874	.49610920
675.00	1.1	-8.0	2.85603	306.9	.03109230	.52720150
663.00	.6	-8.6	2.77761	307.8	.03449149	.56169300
652.00	-.2	-8.6	2.82468	308.4	.03144126	.59313425
641.00	-.6	-10.0	2.52061	309.4	.02999891	.62313317
630.00	-1.2	-10.0	2.56480	310.4	.02854040	.65167357
619.00	-1.7	-11.4	2.30883	311.3	.02735187	.67902544
608.00	-2.4	-12.3	2.16941	312.2	.02513289	.70415834
599.00	-3.0	-14.7	1.76251	312.8	.01805468	.72221301
588.00	-3.5	-14.7	1.79558	313.8	.01996879	.74218181
575.00	-4.2	-15.1	1.77135	315.1	.02365813	.76583993
566.00	-4.8	-15.9	1.67960	315.7	.01584616	.78168610
555.00	-5.3	-15.5	1.77375	316.9	.01938099	.80106708
545.00	-6.1	-14.7	1.93769	317.6	.01893583	.82000291
535.00	-7.1	-15.1	1.90420	318.1	.01960137	.83960429
525.00	-8.1	-15.9	1.81115	318.6	.01895580	.85856009
516.00	-9.2	-18.0	1.51223	318.9	.01526038	.87382047
506.00	-10.0	-18.3	1.49564	319.6	.01534621	.88916668
497.00	-11.2	-20.8	1.19938	319.9	.01237503	.90154171
486.00	-12.4	-21.7	1.12729	320.4	.01305780	.91459951
476.00	-13.6	-22.8	1.03330	320.9	.01102337	.92562288
468.00	-14.8	-22.2	1.10861	320.9	.00874244	.93436532
459.00	-15.9	-21.7	1.19373	321.3	.01057194	.94493726
450.00	-17.7	-21.9	1.18539	320.9	.01092449	.95586175
440.00	-18.8	-21.4	1.28096	321.6	.01258337	.96844512
431.00	-20.2	-22.5	1.17154	321.7	.01126143	.97970656
423.00	-21.5	-22.8	1.16301	321.8	.00952870	.98923525
414.00	-22.9	-23.0	1.15688	322.0	.01065247	.99988772
406.00	-23.9	-23.0	1.17971	322.5	.00953706	1.00942478
397.50	-25.0	-23.8	1.11467	323.0	.00995009	1.01937486
389.00	-26.1	-24.8	1.03088	323.6	.00930461	1.02867948
382.00	-27.0	-26.0	.93065	324.1	.00700541	1.03568488
374.00	-28.2	-26.7	.88633	324.5	.00741620	1.04310109
366.00	-29.5	-28.5	.75763	324.7	.00670999	1.04981108
358.00	-30.8	-30.1	.65520	325.0	.00576660	1.05557768
350.00	-32.2	-31.4	.58255	325.3	.00505202	1.06062970
343.00	-33.1	-33.2	.49204	325.8	.00383779	1.06446749
335.00	-34.4	-36.5	.35025	326.3	.00343786	1.06790535
329.00	-35.4	-37.9	.30848	326.7	.00201650	1.06992185
321.00	-36.5	-38.6	.29249	327.4	.00245292	1.07237478
315.00	-37.8	-37.1	.34891	327.3	.00196345	1.07433823
308.00	-39.3	-38.7	.30030	327.4	.00231859	1.07665682
301.00	-40.4	-40.5	.24935	328.0	.00196303	1.07861985
294.00	-41.8	-42.7	.19843	328.3	.00159921	1.08021906
288.00	-43.1	-44.7	.16171	328.4	.00110248	1.08132154
281.00	-44.4	-46.1	.14067	328.8	.00107995	1.08240148
276.00	-45.4	-47.8	.11645	329.1	.00065592	1.08305740

TABLE VIII

Frost Point Hygrometer Data Rapid City, South Dakota 11/20/68 2005Z Ascent

P(mb)	T(°C)	F(°C)	w(g/kg)	θ(°K)	M(cm)	∑M(cm)
905.00	17.7	-6.8	2.37601	299.3		
894.00	15.9	-6.8	2.40536	298.4	.02683407	.02683407
879.00	14.4	-8.5	2.11082	298.4	.03456244	.06139651
862.00	13.1	-7.6	2.31328	298.7	.03837214	.09976865
830.00	11.7	-6.4	2.69017	300.5	.08168861	.18145727
805.00	10.5	-6.8	2.67243	301.8	.06840026	.24985753
796.00	9.1	-6.8	2.70278	301.3	.02468199	.27453952
783.00	8.1	-6.8	2.74785	301.6	.03615199	.31069151
766.00	6.9	-7.6	2.60441	302.2	.04642245	.34711396
753.00	6.5	-14.8	1.39390	303.3	.02651927	.38363323
737.00	5.8	-20.9	.79595	304.3	.01787625	.40150948
723.00	5.2	-20.2	.86894	305.4	.01189202	.41340150
708.00	4.5	-20.7	.84741	306.4	.01313527	.42653677
697.00	3.8	-26.4	.49143	307.0	.00751385	.43405062
681.00	2.9	-27.1	.46696	308.1	.00782353	.44187415
671.00	2.1	-24.0	.64619	308.5	.00567928	.44755343
659.00	1.5	-23.6	.68555	309.5	.00815345	.45570688
648.00	.7	-24.4	.64257	310.0	.00745371	.46316059
637.00	.3	-26.6	.52760	311.1	.00656728	.46972787
628.00	.2	-23.8	.70502	312.2	.00565997	.47538784
617.00	-.5	-22.3	.83195	313.0	.00862582	.48401366
606.00	-1.3	-19.0	1.16849	313.7	.01122694	.49524060
592.00	-2.5	-17.1	1.42834	314.4	.01854874	.51378934
583.00	-3.1	-21.2	.98368	315.1	.01107557	.52486491
570.00	-4.1	-27.5	.53761	315.9	.01009017	.53495508
558.00	-5.2	-29.9	.42996	316.6	.00592387	.54087895
547.00	-6.7	-30.5	.41045	316.6	.00471653	.54559548
535.00	-7.7	-30.3	.42649	317.4	.00512405	.55071953
523.00	-9.1	-26.2	.66784	317.7	.00669993	.55741946
514.00	-10.3	-17.9	1.52311	317.9	.01006043	.56747989
502.00	-11.9	-17.7	1.59884	318.1	.01911388	.58659378
492.00	-13.2	-19.0	1.43987	318.4	.01550356	.60209733
481.00	-14.6	-18.5	1.54843	318.7	.01677102	.61886835
471.00	-15.8	-19.0	1.50422	319.1	.01557471	.63444306
460.00	-17.3	-20.5	1.33604	319.4	.01594019	.65038325
451.00	-18.6	-20.9	1.30176	319.6	.01211227	.66249552
440.00	-20.0	-20.9	1.33437	320.1	.01479451	.67729004
431.00	-20.8	-21.4	1.30120	320.9	.01210204	.68939207
420.00	-22.1	-22.5	1.19629	321.7	.01401646	.70340854
410.00	-23.1	-23.2	1.15040	322.6	.01197286	.71538140
400.00	-24.9	-24.0	1.08474	322.6	.01140374	.72678514
392.00	-26.2	-25.2	.98179	322.8	.00843480	.73521994
382.00	-27.2	-28.0	.76069	323.8	.00889020	.74411014
372.00	-28.8	-29.2	.69044	324.2	.00740373	.75151387
362.00	-30.5	-30.8	.60006	324.4	.00658420	.75809807
353.00	-31.7	-32.0	.54164	325.1	.00524248	.76334055
343.00	-33.3	-33.9	.45704	325.6	.00509529	.76843584
335.00	-34.7	-36.0	.37178	325.9	.00338295	.77181879
326.00	-36.7	-38.6	.28828	325.8	.00303091	.77484970
318.00	-37.8	-40.3	.24134	326.5	.00216171	.77701141
310.00	-39.4	-41.9	.20647	326.6	.00182779	.77883920

TABLE IX

Frost Point Hygrometer Data Rapid City, South Dakota 11/20/68 2005Z Descent

P(mb)	T(°C)	F(°C)	w(g/kg)	θ(°K)	M(cm)	∑M(cm)
866.00	14.9	-3.5	3.28828	300.2		
852.00	13.8	-3.5	3.34260	300.4	.04736324	.04736324
840.00	12.8	-3.5	3.39061	300.6	.04122360	.08858684
829.00	11.9	-3.5	3.43585	300.7	.03831165	.12689848
820.00	11.0	-3.5	3.47377	300.7	.03172775	.15862623
810.00	10.0	-3.5	3.51690	300.8	.03566657	.19429280
798.00	9.4	-3.5	3.57009	301.4	.04338957	.23768237
786.00	8.7	-4.5	3.33436	301.9	.04227194	.27995431
775.00	8.1	-7.2	2.67275	302.5	.03371319	.31366751
765.00	7.7	-11.1	1.91421	303.2	.02340275	.33707026
756.00	7.2	-13.5	1.56013	303.7	.01595351	.35302377
745.00	6.8	-18.5	.99885	304.5	.01436152	.36738528
737.00	6.5	-20.5	.83322	305.1	.00747779	.37486307
727.00	6.2	-23.6	.62136	306.0	.00742130	.38228437
717.00	5.9	-25.6	.51556	306.9	.00580059	.38808496
709.00	5.2	-26.4	.48311	307.1	.00407607	.39216113
695.00	4.5	-26.4	.49285	308.0	.00697105	.39913218
686.00	3.6	-26.6	.48989	308.2	.00451253	.40364471
678.00	2.9	-26.8	.48672	308.5	.00398614	.40763085
669.00	2.2	-27.3	.46655	308.9	.00437725	.41200809
659.00	1.5	-27.7	.45680	309.5	.00471096	.41671905
650.00	.6	-27.8	.45473	309.6	.00418554	.42090459
640.00	-.2	-26.6	.52513	310.0	.00499922	.42590381
631.00	-1.1	-27.1	.50399	310.4	.00472550	.43062931
622.00	-1.2	-28.9	.42753	311.5	.00427736	.43490668
615.00	-1.2	-29.2	.41745	312.5	.00301778	.43792446
606.00	-1.6	-22.8	.81145	313.3	.00564289	.44356735
596.00	-2.3	-19.2	1.16022	314.1	.01005951	.45362686
589.00	-3.1	-18.5	1.26393	314.2	.00865766	.46228452
580.00	-3.7	-16.8	1.49576	314.8	.01267199	.47495651
572.00	-4.4	-16.6	1.55823	315.3	.01246519	.48742171
565.00	-4.9	-16.6	1.57758	315.8	.01119928	.49862099
558.00	-5.8	-16.8	1.55488	315.9	.01118731	.50980830
550.00	-7.0	-17.1	1.53768	315.8	.01262264	.52243094
541.00	-7.9	-17.1	1.56333	316.2	.01423928	.53667022
534.00	-8.9	-17.7	1.50280	316.2	.01095042	.54762064
526.00	-9.8	-18.5	1.41566	316.4	.01191203	.55953267
520.00	-10.8	-17.9	1.50549	316.3	.00894226	.56847493
513.00	-11.3	-16.6	1.73794	316.9	.01158363	.58005856
507.00	-12.1	-16.3	1.80495	317.0	.01084554	.59090410
501.00	-12.7	-16.0	1.87756	317.3	.01127295	.60217705
495.00	-13.7	-15.7	1.95373	317.2	.01172838	.61390543
489.00	-14.3	-15.7	1.97777	317.5	.01203515	.62594058
481.00	-15.2	-16.3	1.90282	318.0	.01583907	.64177965
474.00	-15.9	-17.1	1.78494	318.4	.01317050	.65495014
466.00	-16.9	-17.7	1.72270	318.7	.01431683	.66926697
460.00	-17.6	-17.9	1.70240	319.1	.01049493	.67975190
452.00	-18.4	-18.7	1.60708	319.6	.01350801	.69325991
446.00	-19.3	-19.0	1.58875	319.7	.00978312	.70304303
438.00	-20.3	-19.5	1.54161	320.1	.01277696	.71581998
431.00	-21.1	-19.7	1.53070	320.6	.01097251	.72679250
423.00	-22.3	-20.0	1.52257	320.7	.01246230	.73925480
416.00	-23.2	-20.5	1.47769	321.1	.01071517	.74996997
409.00	-24.3	-20.9	1.43574	321.3	.01040506	.76037504
402.00	-25.1	-23.2	1.17334	321.8	.00931808	.76969312
396.00	-26.2	-24.2	1.07404	321.8	.00687967	.77657279
388.00	-26.9	-24.6	1.05225	322.7	.00867867	.78525147
381.00	-27.7	-27.1	.83513	323.3	.00674061	.79199208
374.00	-28.6	-29.0	.69894	323.9	.00547880	.79747088
367.00	-29.7	-29.7	.66532	324.2	.00487232	.80234320
361.00	-30.6	-30.3	.63226	324.5	.00397216	.80631536
355.00	-31.7	-32.8	.49834	324.6	.00346099	.80977635
350.00	-32.5	-34.4	.42216	324.8	.00234820	.81212455
344.00	-33.4	-35.6	.37763	325.2	.00244832	.81457287
338.00	-34.4	-36.6	.34391	325.5	.00220877	.81678164
331.00	-35.5	-37.0	.33711	325.9	.00243218	.81921382
326.00	-36.7	-37.0	.34228	325.8	.00173312	.82094695
320.00	-37.5	-37.5	.33051	326.3	.00205955	.82300650
314.00	-38.4	-43.1	.17918	326.9	.00156027	.82456677
309.00	-39.7	-45.0	.14525	326.5	.00082763	.82539439
303.50	-40.5	-46.0	.13115	327.2	.00077561	.82617000
299.00	y41.5	-47.2	.11582	327.1	.00056702	.82673702
294.00	-42.7	-48.0	.10605	326.9	.00056599	.82730301
288.00	-44.2	-48.1	.10712	326.8	.00065257	.82795557
283.00	-44.7	-48.3	.10678	327:7	.00054568	.82850125
278.00	-46.0	-50.0	.08774	327.5	.00049624	.82899749
273.00	-46.6	-50.9	.08003	328.2	.00042798	.82942547
267.00	-47.8	-51.9	.07269	328.6	.00046748	.82989295
263.00	-48.7	-52.3	.07027	328.7	.00029173	.83018468
258.00	-49.8	-52.7	.06756	329.0	.00035159	.83053628
254.00	-51.0	-53.8	.05995	328.6	.00026022	.83079650
249.00	-52.0	-55.4	.04960	329.0	.00027946	.83107595
244.00	-52.9	-56.3	.04518	329.5	.00024177	.83131772
239.00	-53.7	-57.1	.04161	330.3	.00022139	.83153911
234.00	-54.3	-57.8	.03870	331.4	.00020486	.83174397
229.00	-54.9	-58.1	.03774	332.5	.00019500	.83193897
224.00	-55.5	-58.8	.03547	333.7	.00018676	.83212572
219.00	-56.2	-60.2	.02986	334.9	.00016665	.83229238
215.00	-57.0	-61.2	.02670	335.3	.00011542	.83240780
210.00	-57.2	-62.2	.02226	337.2	.00012483	.83253269
205.50	-57.7	-64.1	.01849	338.7	.00009356	.83262625
201.00	-57.9	-64.7	.01736	340.4	.00008231	.83270857
197.00	-58.1	-65.9	.01504	342.1	.00006613	.83277470
192.00	-58.3	-67.2	.01283	344.2	.00007111	.83284581
188.00	-58.3	-68.1	.01141	346.3	.00004947	.83289528
184.00	-59.0	-69.0	.01023	347.3	.00004415	.83293943
180.00	-59.5	-70.0	.00906	348.8	.00003935	.83297879
176.00	-59.5	-71.1	.00784	350.3	.00003447	.83301325
172.50	-60.2	-71.5	.00758	351.9	.00002752	.83304077
168.00	-61.6	-71.9	.00730	352.1	.00003414	.83307491
165.00	-62.9	-72.2	.00711	351.8	.00002205	.83309697
161.00	-64.2	-72.5	.00690	352.1	.00002860	.83312556
157.00	-64.2	-73.1	.00648	354.6	.00002730	.83315286
153.00	-64.5	-74.7	.00523	356.8	.00002389	.83317675
149.00	-64.7	-76.8	.00383	359.0	.00001846	.83319521
146.00	-65.6	-78.3	.00309	359.7	.00001058	.83320579
142.00	-66.7	-79.1	.00278	360.6	.00001198	.83321777
139.00	-67.0	-79.9	.00250	362.3	.00000808	.83322585
135.00	-66.7	-80.3	.00240	365.8	.00001000	.83323584
132.00	-66.4	-80.3	.00245	368.7	.00000742	.83324327
129.00	-66.1	-80.3	.00251	371.6	.00000760	.83325087
126.00	-66.7	-80.5	.00246	373.1	.00000761	.83325848
122.50	-67.0	-80.8	.00242	375.6	.00000872	.83326720
120.00	-67.0	-80.8	.00247	377.8	.00000624	.83327344
118.00	-66.7	-80.6	.00259	380.2	.00000516	.83327860
114.00	-65.9	-80.3	.00284	385.5	.00001109	.83328968
111.00	-65.0	-79.9	.00309	390.1	.00000907	.83329876
108.00	-64.5	-79.7	.00332	394.1	.00000980	.83330856
105.50	-64.2	-79.7	.00340	397.3	.00000855	.83331712
102.50	-64.2	-79.8	.00344	400.6	.00001046	.83332758
100.00	-64.5	-80.8	.00338	402.9	.00000870	.83333628
97.00	-64.7	-80.3	.00334	405.9	.00001028	.83334656
94.90	-65.0	-80.4	.00337	407.9	.00000718	.83335374
92.00	-65.0	-80.5	.00342	411.5	.00001004	.83336379
89.50	-65.3	-80.6	.00347	414.2	.00000878	.83337256
87.00	-65.3	-80.7	.00346	417.6	.00000884	.83338140
84.90	-65.6	-80.9	.00345	420.0	.00000739	.83338879
82.50	-65.9	-81.3	.00334	422.9	.00000830	.83339709
79.90	-65.6	-81.6	.00324	427.3	.00000873	.83340582
77.50	-65.3	-82.1	.00310	431.6	.00000776	.83341359
75.00	-64.5	-82.1	.00320	437.4	.00000802	.83342160
73.00	-63.7	-82.2	.00324	442.5	.00000656	.83342816
71.80	-62.6	-82.3	.00324	446.8	.00000396	.83343212
68.50	-61.9	-82.5	.00329	454.5	.00001098	.83344311
66.30	-60.9	-82.7	.00329	460.9	.00000738	.83345048
64.00	-60.2	-83.0	.00325	467.1	.00000766	.83345814
62.30	-59.7	-83.1	.00328	471.8	.00000566	.83346380
60.00	-59.5	-83.3	.00324	477.4	.00000764	.83347145
58.50	-59.3	-83.5	.00322	481.3	.00000493	.83347638
56.00	-59.3	-83.6	.00331	487.4	.00000831	.83348469
54.00	-59.0	-84.0	.00320	493.0	.00000663	.83349133
52.50	-58.6	-84.1	.00324	498.1	.00000492	.83349624
51.00	-58.3	-84.3	.00322	502.7	.00000493	.83350118
49.40	-58.6	-84.5	.00321	506.8	.00000525	.83350642
47.60	-59.3	-84.6	.00327	510.6	.00000595	.83351237
45.90	-59.5	-85.0	.00321	515.3	.00000562	.83351798
44.50	-59.7	-85.2	.00320	519.4	.00000457	.83352256
43.00	-59.5	-85.3	.00325	525.0	.00000493	.83352749
41.50	-59.3	-85.4	.00331	531.0	.00000501	.83353250
40.20	-58.6	-85.7	.00323	537.5	.00000432	.83353682
38.80	-58.1	-86.0	.00316	544.1	.00000456	.83354138
37.40	-57.9	-86.4	.00309	550.4	.00000446	.83354583
36.20	-57.7	-86.5	.00313	556.2	.00000380	.83354963
34.90	-57.5	-86.8	.00306	562.6	.00000410	.83355373
33.70	-57.2	-86.9	.00311	568.8	.00000377	.83355750
32.40	-57.0	-87.3	.00304	575.8	.00000407	.83356157
31.25	-56.8	-87.5	.00303	582.4	.00000356	.83356513
29.80		-88.0	.00292		.00000440	.83356953
28.50		-88.3	.00286		.00000383	.83357336
27.10		-88.6	.00288		.00000410	.83357745
26.00		-88.9	.00281		.00000319	.83358064
24.60		-89.2	.00284		.00000402	.83358467
23.50		-89.7	.00270		.00000310	.83358777
22.20		-90.4	.00254		.00000347	.83359124
21.00		-91.6*	.00215		.00000286	.83359410
20.00		-91.2	.00242		.00000232	.83359642
19.00		-91.8	.00229		.00000240	.83359882
18.20		-92.3	.00214		.00000180	.83360063
17.40		-92.4*	.00223		.00000177	.83360240
16.70		-92.8*	.00215		.00000156	.83360396
16.10		-92.5	.00236		.00000137	.83360533
15.50		-93.1	.00218		.00000139	.83360672
14.95		-93.3	.00219		.00000122	.83360794
14.40		-93.3	.00228		.00000125	.83360919
14.00		-93.4	.00228		.00000092	.83361012
13.50		-93.4	.00236		.00000118	.83361129
13.15		-93.6	.00235		.00000083	.83361213
12.80		-93.6	.00241		.00000085	.83361298
12.50		-93.6	.00247		.00000075	.83361372
12.20		-94.7	.00203		.00000069	.83361441
11.90		-94.7	.00308		.00000063	.83361503
11.60		-94.7	.00214		.00000064	.83361568
11.40		-96.0	.00171		.00000039	.83361606
11.20		-96.2	.00168		.00000034	.83361641
11.00		-95.8	.00183		.00000036	.83361676
10.80		-95.3	.00207		.00000039	.83361715
10.70		-95.1	.00217		.00000021	.83361736

D. MRIR 0.2-4.0μm Channel Data.

Earth reflectance data have been determined from the MRIR 0.2-4.0μm channel data. The quantity measured is the bi-directional reflectance $\rho(\theta_o, \phi_o, \theta, \phi)$, where θ_o, ϕ_o are the zenith and azimuth angles of the incident ray and θ, ϕ are the zenith and azimuth angles of the reflected ray. The geometry is illustrated by figure 32. The azimuth angle $\psi = \phi - \phi_o$ is used instead of ϕ, thus: $\rho(\theta_o, \phi_o, \theta, \psi)$.

The sun angles θ_o and ϕ_s (the azimuth angle of the sun, measured clockwise from north, not the same as ϕ_o) are calculated from:

$$\cos\theta_o = \sin\phi' \sin\delta + \cos\phi' \cos\delta \cos H$$

$$\sin\phi_s = \frac{\cos\delta \cdot \sin H}{\sin\theta_o}$$

where

ϕ' = the latitude of the sub-balloon point

δ = the sun's declination (from Air Almanac)

$H = GHA - \lambda$

GHA= Greenwich hour angle of the sun (from Air Almanac)

λ = longitude of the sub-balloon point

Sun angle data for this balloon flight are given in table X, which is the computer print out for the calculations indicated above. The elevation angle of the sun (El), and the azimuth angle of the sun (Az), measured clockwise from the south are given as a function of time (MST).

thus:

$$\theta = 90 - El$$

$$\phi_s = Az - 180$$

where ϕ_s is measured clockwise from north.

The azimuth of a point on the gondola relative to the sun is measured throughout the flight by a rotating photocell device which is mounted on the top side of the gondola, see figure 33. The photocell receives its signal through a slit which defines a vertical plane. The device is rotated about a vertical axis once every 4.89 seconds. It's position is indicated by a commutator which produces a pulse for every 2 degrees of rotation. The position of a horizontal

TABLE X

Sun Angle Data for 20 November 1968 Balloon Flight

$RUN –LOAD# 5=*SOURCE* 6=*SINK*
EXECUTION BEGINS

MONTH = 11 DAY = 20

MST =	5.00	LAMBDA =	103.18	PHI =	44.04	EL =	-20.36	AZ =	-81.78
MST =	6.00	LAMBDA =	103.18	PHI =	44.04	EL =	-9.89	AZ =	-71.98
MST =	7.00	LAMBDA =	102.75	PHI =	43.45	EL =	0.57	AZ =	-61.59
MST =	7.33	LAMBDA =	102.75	PHI =	43.27	EL =	3.80	AZ =	-58.08
MST =	7.67	LAMBDA =	102.80	PHI =	43.20	EL =	6.83	AZ =	-54.51
MST =	8.00	LAMBDA =	103.08	PHI =	43.17	EL =	9.59	AZ =	-50.98
MST =	8.33	LAMBDA =	103.16	PHI =	43.06	EL =	12.37	AZ =	-47.17
MST =	8.67	LAMBDA =	103.28	PHI =	42.98	EL =	14.96	AZ =	-43.24
MST =	9.00	LAMBDA =	103.30	PHI =	42.92	EL =	17.40	AZ =	-39.07
MST =	9.33	LAMBDA =	103.32	PHI =	42.88	EL =	19.62	AZ =	-34.71
MST =	9.67	LAMBDA =	103.34	PHI =	42.80	EL =	21.64	AZ =	-30.18
MST =	10.00	LAMBDA =	103.35	PHI =	42.75	EL =	23.39	AZ =	-25.45
MST =	10.33	LAMBDA =	103.40	PHI =	42.62	EL =	24.93	AZ =	-20.62
MST =	10.67	LAMBDA =	103.44	PHI =	42.50	EL =	26.18	AZ =	-15.62
MST =	11.00	LAMBDA =	103.48	PHI =	42.38	EL =	27.12	AZ =	-10.49
MST =	11.33	LAMBDA =	103.48	PHI =	42.24	EL =	27.76	AZ =	-5.23
MST =	11.65	LAMBDA =	103.50	PHI =	42.12	EL =	28.04	AZ =	-0.26
MST =	11.67	LAMBDA =	103.50	PHI =	42.12	EL =	28.04	AZ =	0.06
MST =	11.90	LAMBDA =	103.51	PHI =	42.04	EL =	28.03	AZ =	3.78
MST =	12.00	LAMBDA =	103.52	PHI =	42.00	EL =	27.98	AZ =	5.37
MST =	12.33	LAMBDA =	103.54	PHI =	41.83	EL =	27.64	AZ =	10.65
MST =	12.67	LAMBDA =	103.56	PHI =	41.67	EL =	26.93	AZ =	15.85
MST =	13.00	LAMBDA =	103.60	PHI =	41.50	EL =	25.92	AZ =	20.91
MST =	13.33	LAMBDA =	103.66	PHI =	41.35	EL =	24.59	AZ =	25.81
MST =	13.67	LAMBDA =	103.66	PHI =	41.20	EL =	22.95	AZ =	30.60
MST =	14.00	LAMBDA =	103.64	PHI =	41.10	EL =	20.97	AZ =	35.20
MST =	14.33	LAMBDA =	103.64	PHI =	41.08	EL =	18.70	AZ =	39.57
MST =	15.00	LAMBDA =	103.64	PHI =	41.05	EL =	13.51	AZ =	47.73
MST =	16.00	LAMBDA =	103.64	PHI =	41.05	EL =	4.44	AZ =	58.68

FIOCS–END OF FILE ON 5

line on the gondola, which is in the same direction as the horizontal axis of the MRIR, is indicated by a marker pulse. In addition a pulse is obtained when the vertical plane defined by the slit passes through the sun. A sample of the data obtained is shown in figure 34.

The photocell rotates in a clockwise direction. If we let σ be the angle from the marker pulse to the next sun pulse, then the azimuth of the reference line on the gondola, i. e. the horizontal axis of the MRIR, measured clockwise from north, is given by:

$$\phi_M = \phi_S - \sigma$$

The radiometer scans a vertical plane at right angles to its horizontal axis, therefore the aximuth of the reflected ray recieved by the radiometer is:

$$\gamma_A = \phi_S - \phi_M - 90 = \sigma - 90$$

or

$$\gamma_B = \phi_S - \phi_M + 90 = \sigma + 90$$

where γ_A is the azimuth for the initial or downward portion of the scan and γ_B is the azimuth for the second half or upward portion of the scan.

A plot of ϕ_M vs. eastern standard time for one hour (1400-1500 EST) of the flight is shown in figure 35. The gondola rotation in azimuth tends to damp out after the balloon is at altitude and so a turning moment is applied to the gondola once every hour to increase its rotation. The moment is applied by two jets of nitrogen gas. The resulting increase in rotation typically achieved can be seen in figure 35 at 1449:24 EST.

A portion of the bi-directional reflectance data obtained so far is shown in figures 36-39. An aerial photograph showing a portion of the earth's surface for which this reflectance data apply is shown in figure 40. The peak in the curve of $\rho(\theta_o, \phi_o, \theta, \gamma)$ at $\theta=80$, $\gamma=0$ in figure 36 is associated with the cloud mass at the top right of the photograph.

E. Filter Wedge Spectrometer Data.

As noted in progress report 05863-24-P for the period 1 October 1968-31 December 1968, magnetic tape recordings and Brush recorder records of the analog IR data and comutated housekeeping data were sent to GSFC personnel on 7 December, 1968 for data analysis and interpretation.

Late in January, we were informed that the magnetic tape data had been digitized and that an analysis had been attempted, however the results were not intelligible. Another Brush recorder with a different time scale and recorder gain were desired so that "hand" data processing could be attempted. This recording was made and was sent to GSFC on 31 January.

F. U. of M. Interferometer Data (By L. W. Chaney)

As noted in the progress report 05863-24-P there were 2 problems in the analysis of the interferometer data caused by equipment failures during the balloon flight. The first was associated with the gain switching amplifier in that the quiescent voltages associated with the low and high gain conditions were not equal. A probable offset voltage was established to correct for this error.

The second problem was associated with the commutator used for interferometer housekeeping data. A malfunction in this unit resulted in failure to recieve data on the cold blackbody and bolometer temperatures. In addition, when the other channels were monitored, they were effected in a manner equivalent to having a voltage source with series resistance and another resistor placed in parallel with the voltage being monitored.

The cold blackbody temperature was also monitored in the general gondola housekeeping data and so its temperature is known, although with less accuracy than desired. The bolometer temperature can be assumed to have been 1^{o} C, based on previous experience with the instrument. The warm blackbody data was corrected for the impedance change by reference to data obtained during the flight from other channels. The characteristics of these other channels were known accurately and thus values of the parameters associated with the circuit failure could be calculated. Assuming that the calculated parameters also apply to the warm blackbody channel, corrected values of the warm blackbody temperature were obtained.

In a sample case, the values of blackbody and bolometer temperatures as indicated above were not consistant with the relative radiances obtained for cold and warm blackbody spectra and so a final adjustment of the calibration blackbody temperatures was made to achieve this consistancy. The adjusted values of blackbody temperature were used for calculation of spectra. The estimated uncertainty in the spectral radiances due to the uncertainties in blackbody temperatures is about 4 ergs·cm^{-2}·sec^{-1}·ster^{-1}·μm^{-1} at 15 μm (a precision of about 0.5 ergs·cm^{-2}·sec^{-1}·ster^{-1}·μm^{-1} is required for accurate temperature inversion).

Most of the data obtained during the flight were examined and the best (noise free) scene and calibration interferograms were processed to spectral radiance curves. The results have not yet been evaluated.

III. Medium and High Resolution Measurements of the 15 μm Absorption Band of CO_2

A. Medium Resolution Measurements

The work on medium resolution measurements of the 15 μm band of CO_2 and the technical report describing the results has been completed. This work, which is the PhD thesis of Henry Reichle, Jr., has been approved by his Doctoral Dissertation Committee. The thesis is now being printed in report form (report 05863-17-T) and will be distributed in May.

B. High Resolution Measurements

The work on high resolution measurements of the 15 μm CO_2 band will be carried out on the 1.8 meter Jarrell-Ash spectrometer located at the University's Willow Run Research Laboratories. Modifications of the instrument for this work have been started, as follows.

1. A new grating has been obtained and has been installed. This grating, made by Bausch and Lomb, is 190mm long by 135mm high, has 60 lines per mm, is blazed at 16μm, and will be used in the 1st order in the double pass mode. A resolution of 0.05 cm^{-1} should be achieved.
2. The instrument is being modified to use a Cu:Ge detector instead of a thermocouple. An intiial design using available lenses was found to be inadequate because the "circle of confusion" obtained was too large for the available detector. The final design uses an an elliptical minor.
3. The instrument is being converted to vacuum operation.

IV. Determination of the Vertical Distribution of O_3 from Radiance Measurements in the 9.6 μm Band (by J. M. Russell)

A study was undertaken to determine the dependance of the weighting functions for the 9.6μ region on instrument viewing direction and resolution. Calculations were performed using a line-by-line integration program developed at this laboratory and they included a range of resolution from 5 cm^{-1} to .2 cm^{-1} and zenith angles rangeing from 0^o to 75^o. The results indicate that there is very little decrease in the amount of overlap of the weighting functions for resolutions down to 2.5 cm^{-1} and there is no great improvement even for the presently unattainable resolution of .2 cm^{-1}. Also, data from the zenith angle scan indicates that there is essentially no improvement in the degree of overlap of the weighting functions from 0^o up to 60^o and only a slight improvement at 75^o.

It is recognized of course, that the weighting functions do not reveal how much independent information is available in the radiance data. Currently an eigenvector analysis of the problem is in progress in an attempt to determine this information.

V. Laboratory Tests of the IRIS Interferometer (by L. W. Chaney)

Examination of the instrument after the balloon flight revealed that some of the instrument cables had been damaged during recovery. These cables were replaced. The instrument was taken to Texas Instruments and completely checked out.

The instrument field of view was then determined using a pin hole mask and hot target arrangement. The results are shown in figure 41. The field of view is defined by three curves of constant intensity. In the figure, the circle corresponds to the theoretical 4 degree half angle field of view of the instrument. The three contours having relative intensities of 30, 80, 300 respectively have their centers displaced slightly from the theoretical center of the field of view.

Next, the instrument was placed in an evironmental test chamber for calibration purposes. At this point work was suspended for about six weeks because the technician most skilled at carrying out this work suffered a heart attack.

VI. The Study of Techniques for Measuring Molecular Collision Rates

A literature search is being made on the status of theoretical studies and experimental measurements of relaxation times because of their great importance to an understanding of the atmospheric heat budget.

Relaxation times are generally defined at atmosphere pressure and room temperature. Although the manner in which they vary as a function of pressure is no great problem, since relaxation time and pressure vary inversely, variation with temperature is much more uncertain. Theoretical calculations indicate that the temperature variation may be very large, however there is no experimental verification at low temperatures. The influence of foreign gases on relaxation times is also very important and experimental data is also needed.

The spectrophone is the instrument most often used for relaxation times. Study has indicated that obvious improvements in the experimental technique can be made, so that accurate low temperature measurements of relaxation times can be made.

VII. Microwave Occultation Studies (by F. F. Fischbach)

Technical Report 05863-16-T, "Analysis of Microwave Occultation Techniques for Atmospheric Soundings" was written and published. This report contained information relative to the microwave inversion process which bears heavily on the Stanford University proposal, and interestingly, on the Mariner flights to Mars and Venus. It suggests that a non-approximate method was in fact available to planetary occultation data reduction but does not conclude that a significant error attaches to the published results. That possibility is not eliminated by the present analysis because no effort has been expended in the analysis of planetary probe data.

A complete mathematical formulation of the Abel transform and its application to earth occultation techniques at both microwave and optical wavelengths is given in an appendix.

Also included is the discussion of a theoretical paper on microwave inversion which contains an error in an important section. This discussion was submitted to the Journal of Geophysical Research and is now under review.

During the report period the study of water vapor asphericity was concluded by the analysis of a case in the literature in which the refractivity at the surface was described by a parabolic function of distance. Our conclusion was that the Stanford technique of analyzing this problem had little

meaning because of the omission of second order spatial derivatives of air density and scale height.

The problem of interpretation of Earth-moon occultation data contained on digital tape output of the ATS-1 spin-scan camera system was referred to computer format specialists at the University of Wisconsin. When the data problem is resolved, the reflected radiation values for lunar features will serve as the refraction input to recover profiles of atmospheric density

A thorough reveiw of the Abelian inversion technique and error analysis previously done for the stellar-refraction case has been completed as necessary preparation for the microwave phase-delay data inversion and error analysis. The latter analysis is underway.

Contribution was made to the paper by Dr. M. A. Alaka, "Theoretical and Practical Considerations for Network Design," presented at the Symposium on Meteorological Observations and Instrumentation, Washington, D. C., February 10-14, 1969.

VIII. Reports Published

Two technical reports were written during this work period, they are:

1. M. F. Graves and F. F. Fischbach "Analysis of Microwave Occultation Techniques for Atmospheric Soundings," Report 05863-16-T, University of Michigan, High Altitude Engineering Laboratory, Contract No. NASr-54(03), January, 1969.
2. H. G. Reichle, Jr. "The Effect of Several Infrared Broadening Gases on the Absorption of Infrared Radiation in the 15 μm Band of Carbon Dioxide," Report 05863-17-T, University of Michigan, High Altitude Engineering Laboratory, Contract No. NASr-54(03). To be distributed in May 1969.

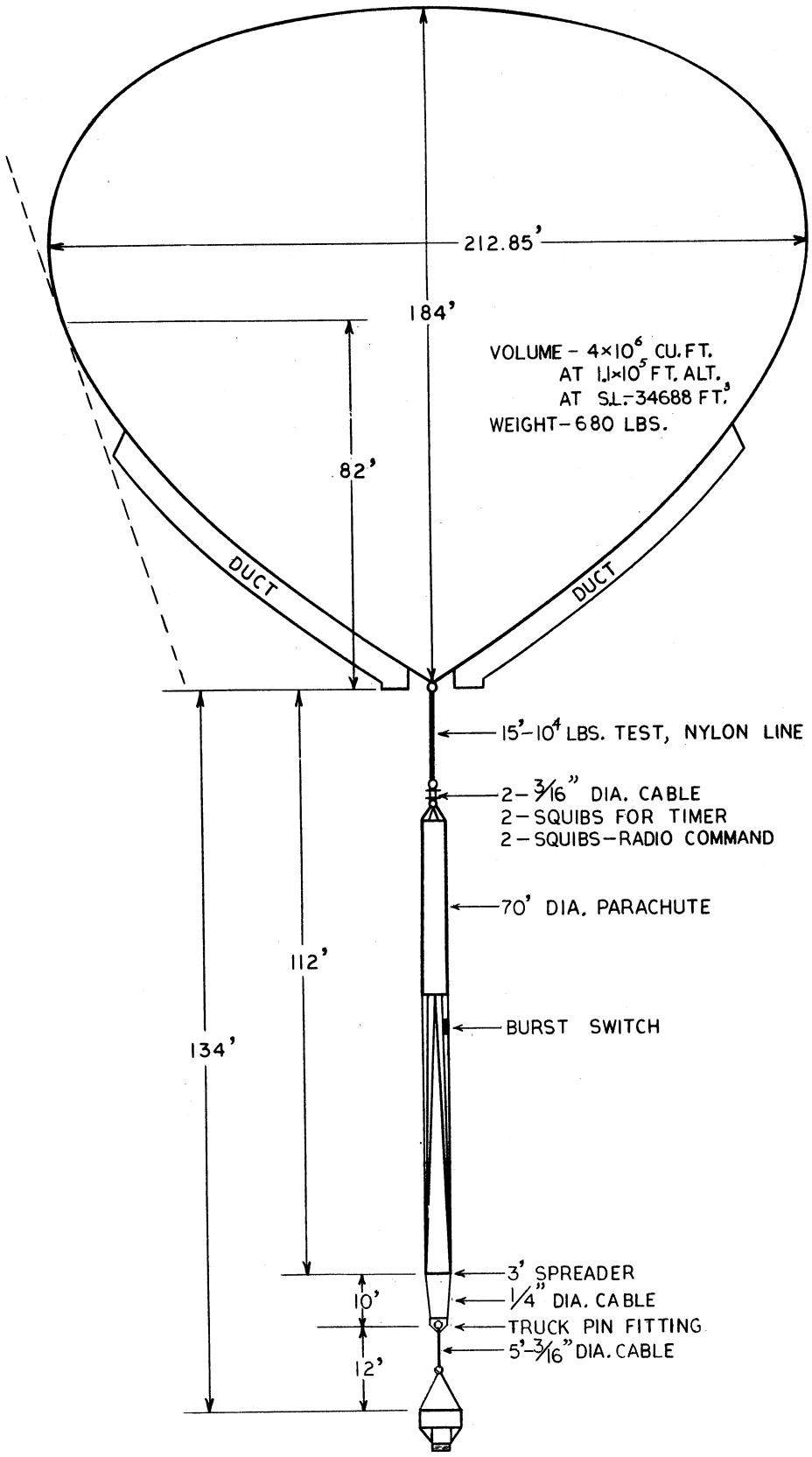

Figure 1. Balloon Configuration, 20 November 1968 Balloon Flight

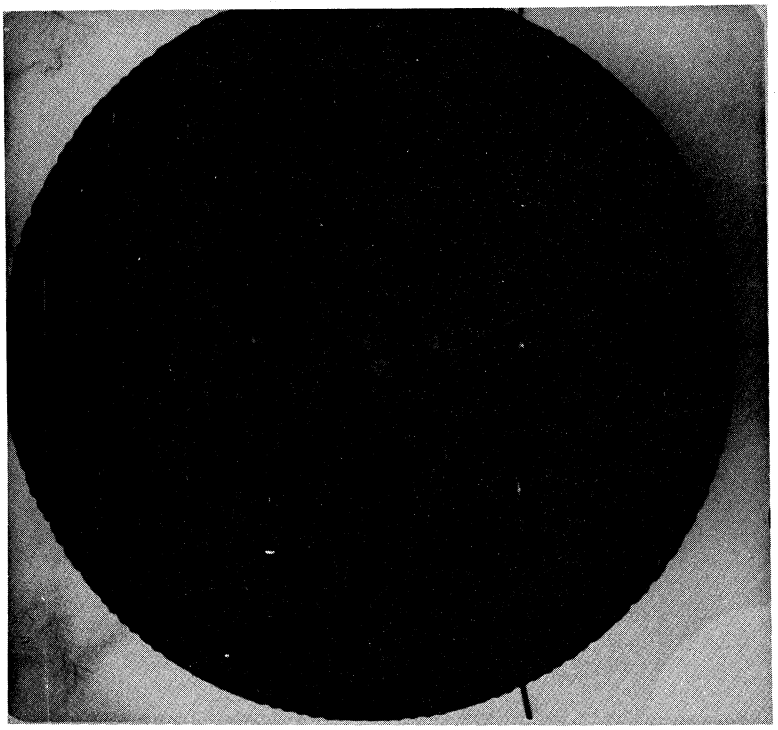

Figure 4. Balloon as Viewed from Balloon Gondola

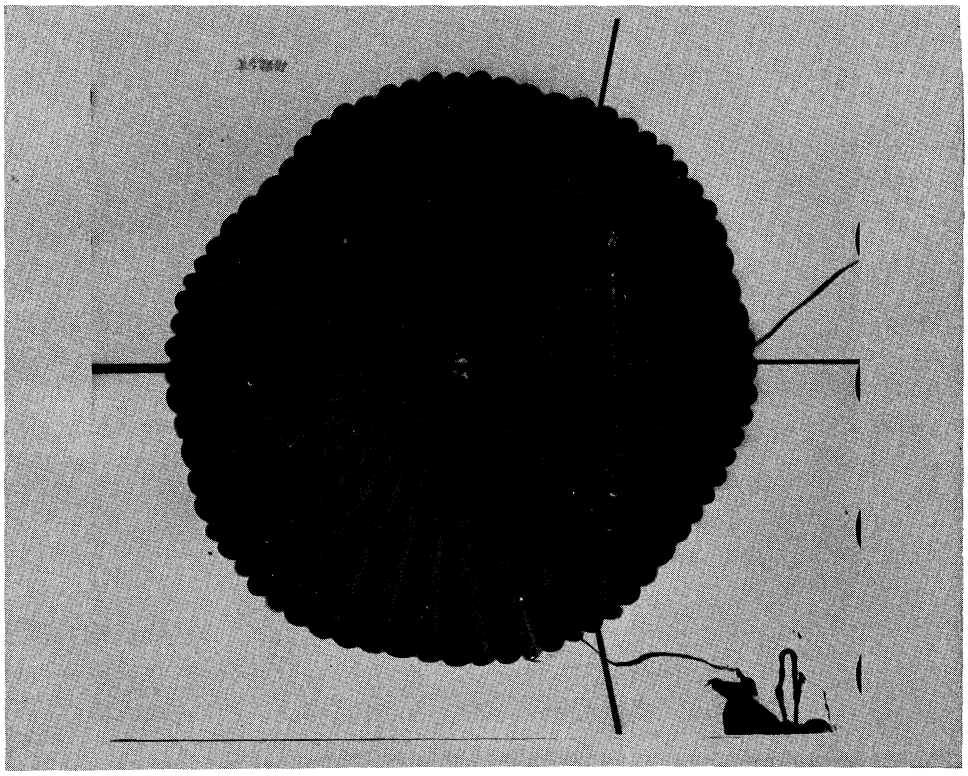

Figure 5. Parachute as Viewed from Balloon Gondola

Figure 6. Photograph 190 Taken by Camera #1 at 1210:15 E. S. T.

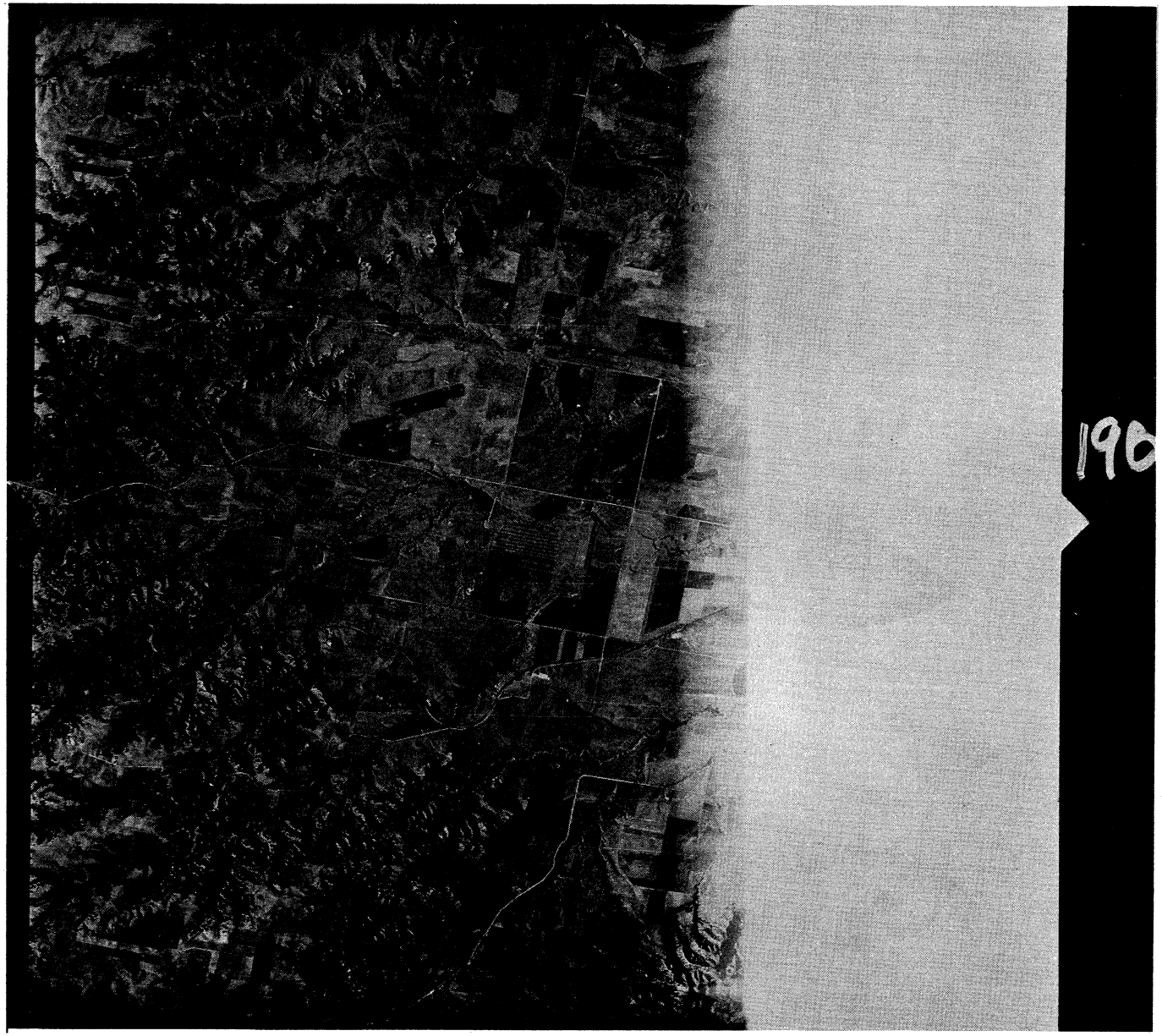

Figure 7. Photograph 190 Taken by Camera #2 at 1210:15 E. S. T.

Figure 8. Photograph 75 Taken by Camera #3 at 1207:03 E. S. T.

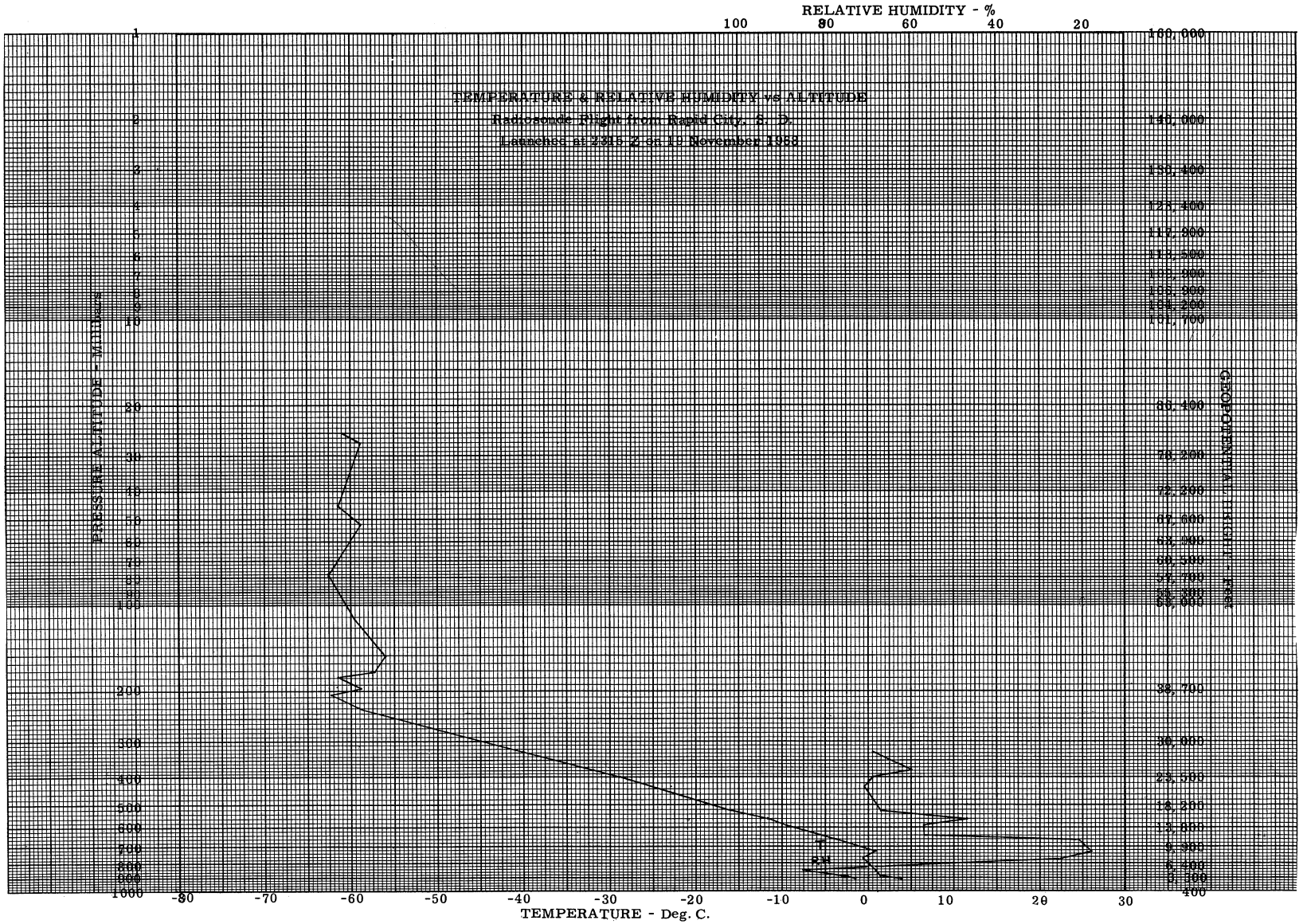

Figure 9. Temperature and Relative Humidity vs. Altitude, Rapid City, South Dakota, 2315Z, 19 November 1968.

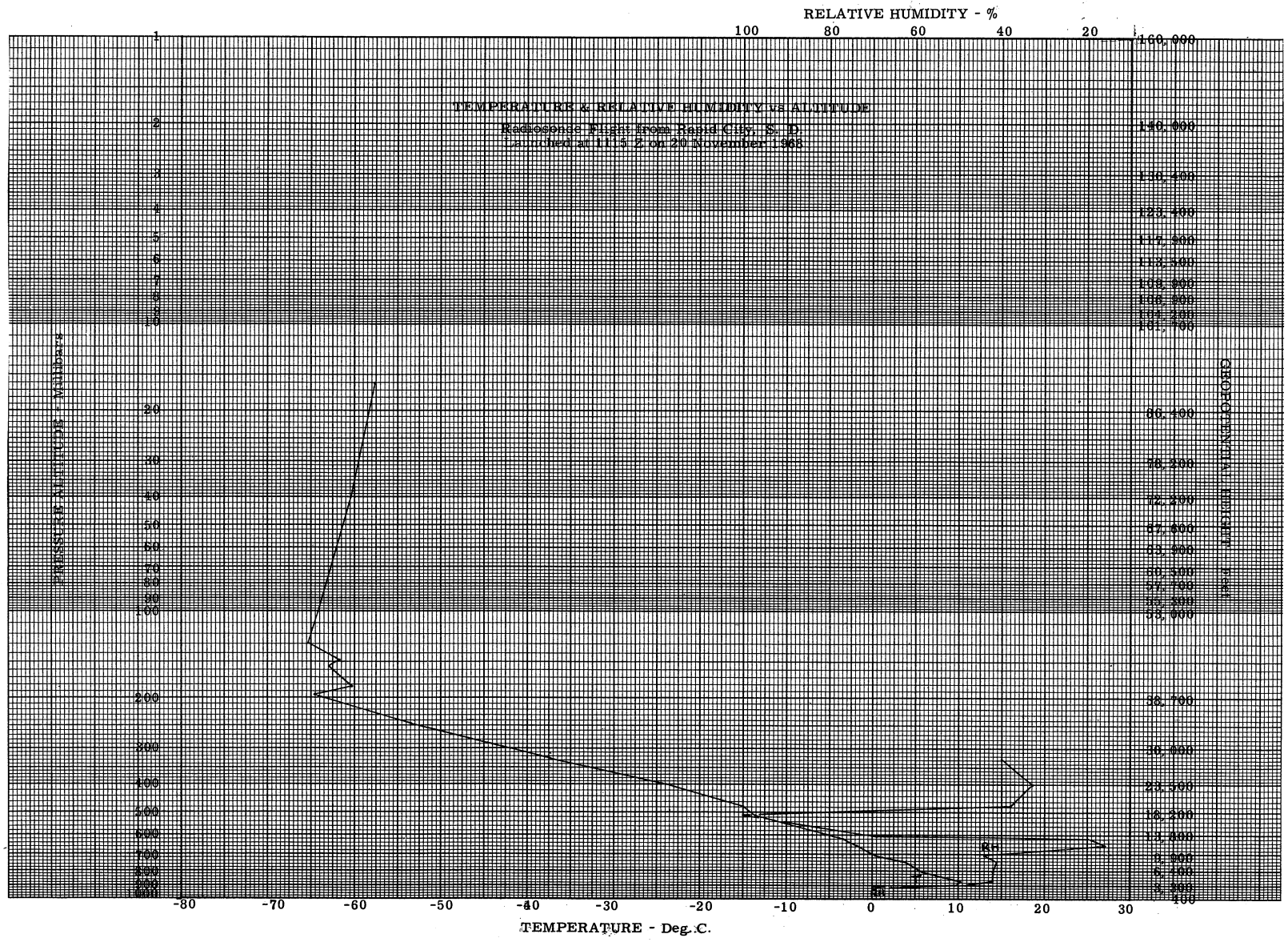

Figure 10. Temperature and Relative Humidity vs. Altitude, Rapid City, South Dakota, 1115Z, 20 November 1968.

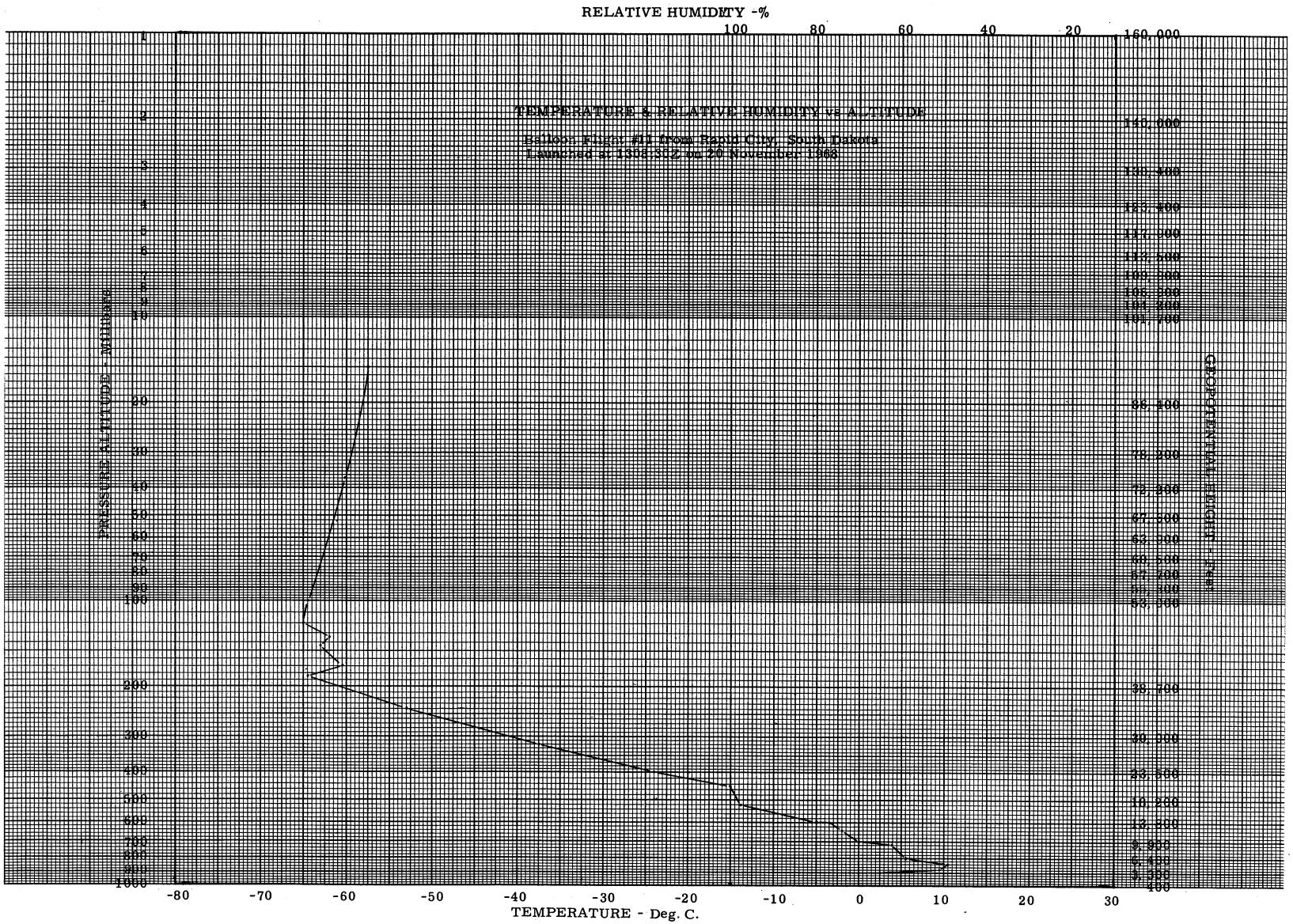

Figure 11. Temperature and Relative Humidity vs. Altitude, Rapid City, South Dakota, 1308 Z, 20 November 1968.

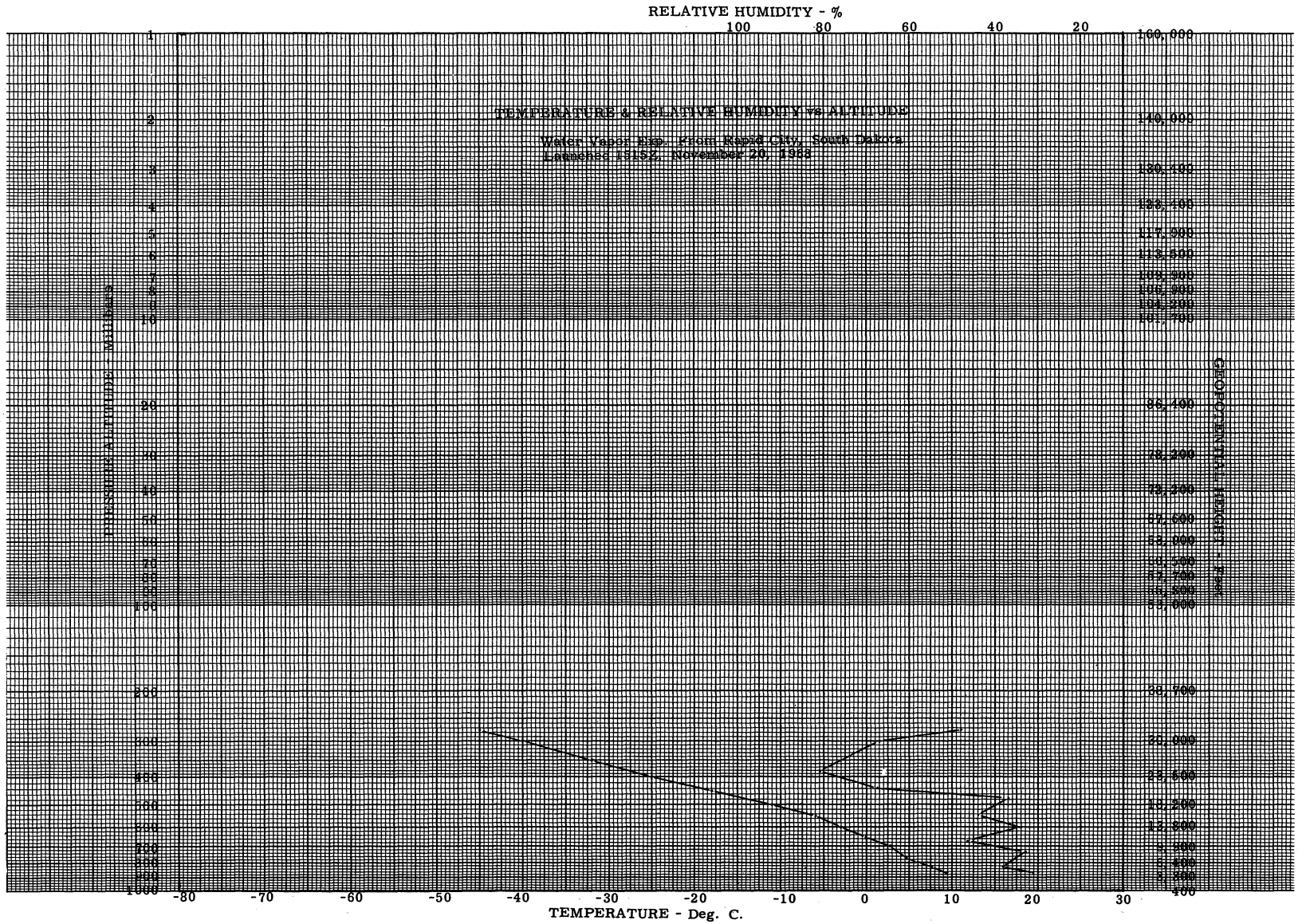

Figure 12. Temperature and Relative Humidity vs. Altitude, Rapid City , South Dakota, 1515Z, 20 November 1968.

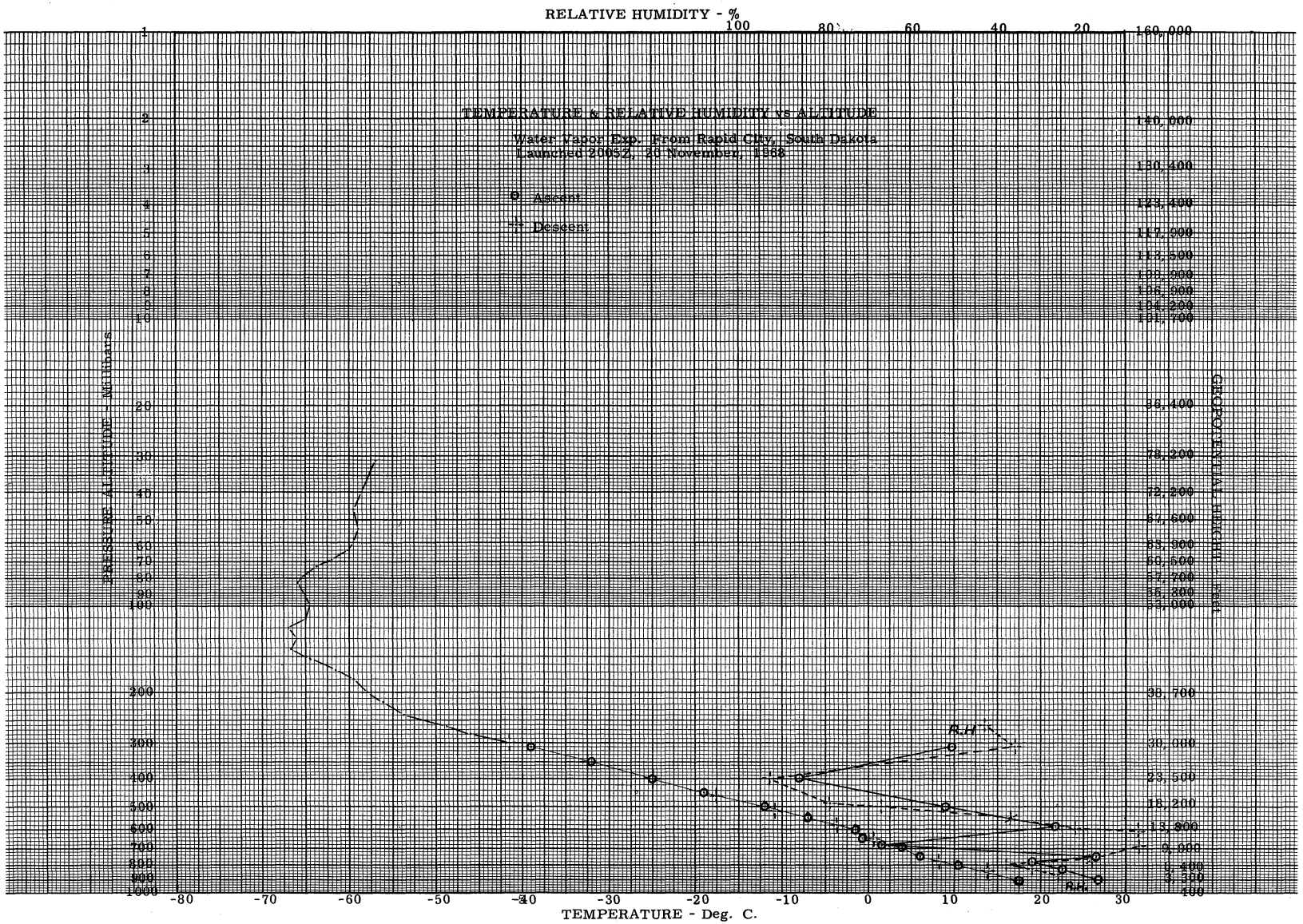

Figure 13. Temperature and Relative Humidity vs. Altitude, Rapid City, South Dakota, 2005Z, 20 November 1968.

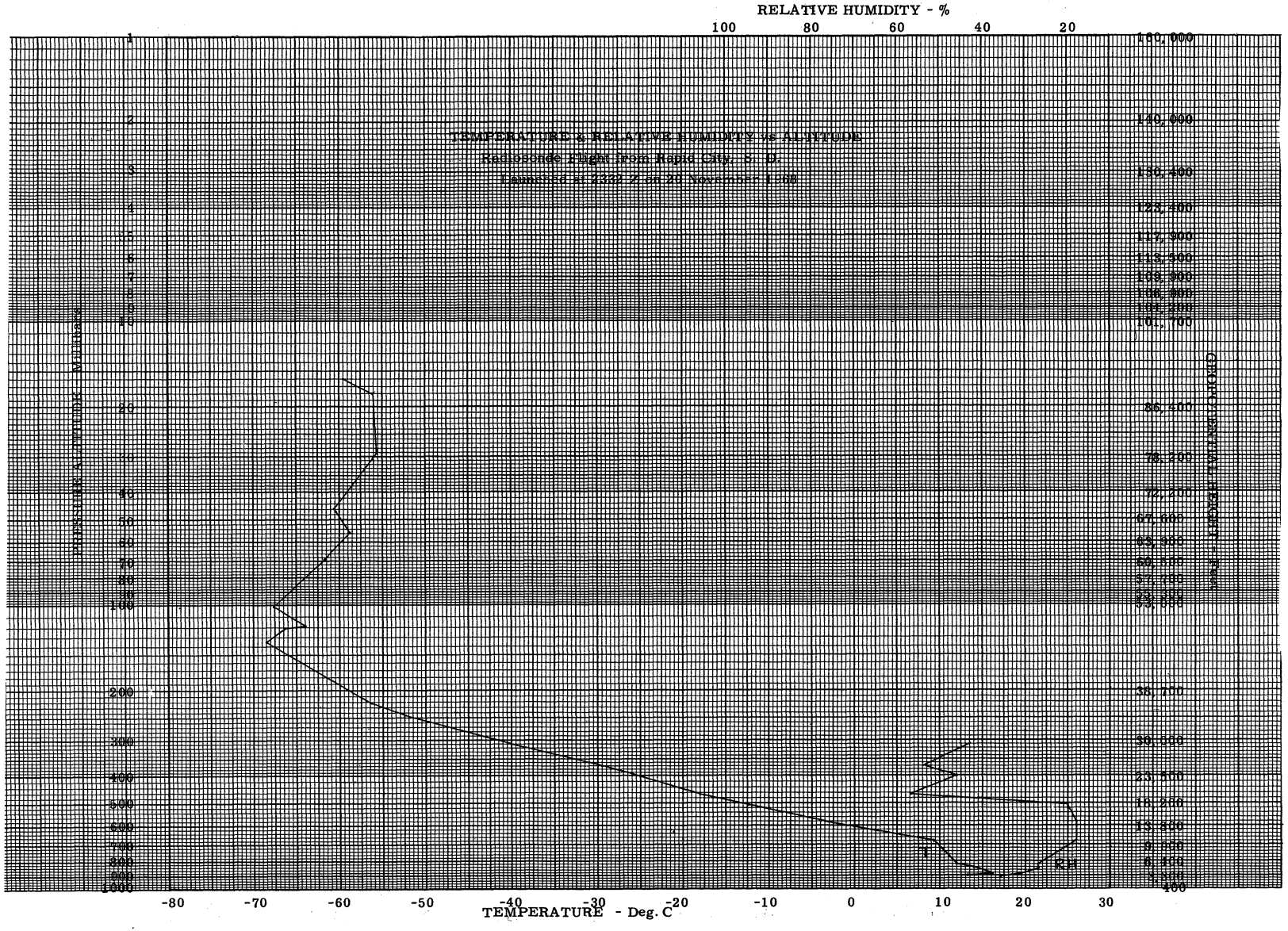

Figure 14. Temperature and Relative Humidity vs. Altitude, Rapid City, South Dakota, 2332Z, 20 November 1968.

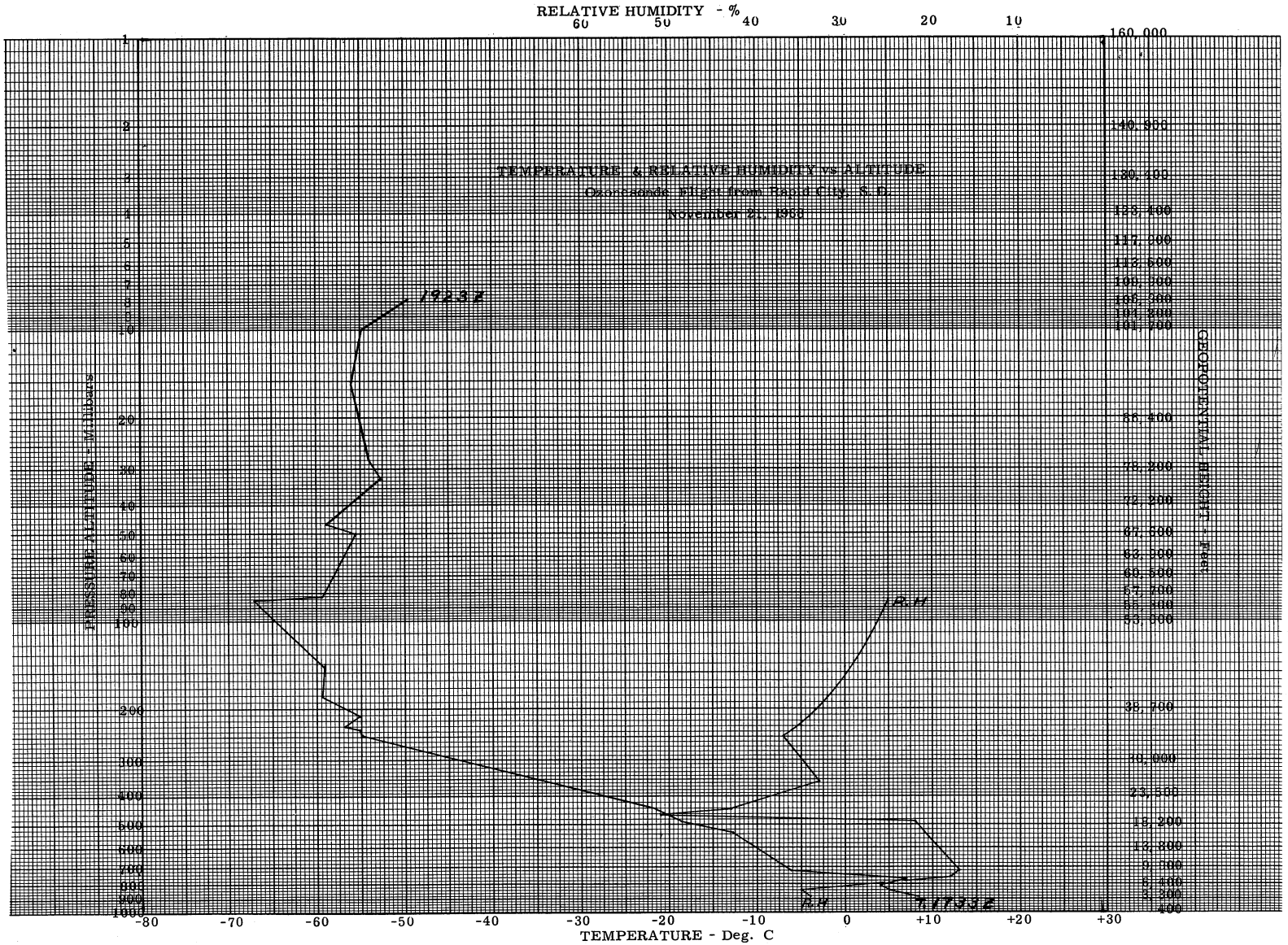

Figure 15. Temperature and Relative Humidity vs. Altitude, Rapid City, South Dakota, 1733Z, 21 November 1968.

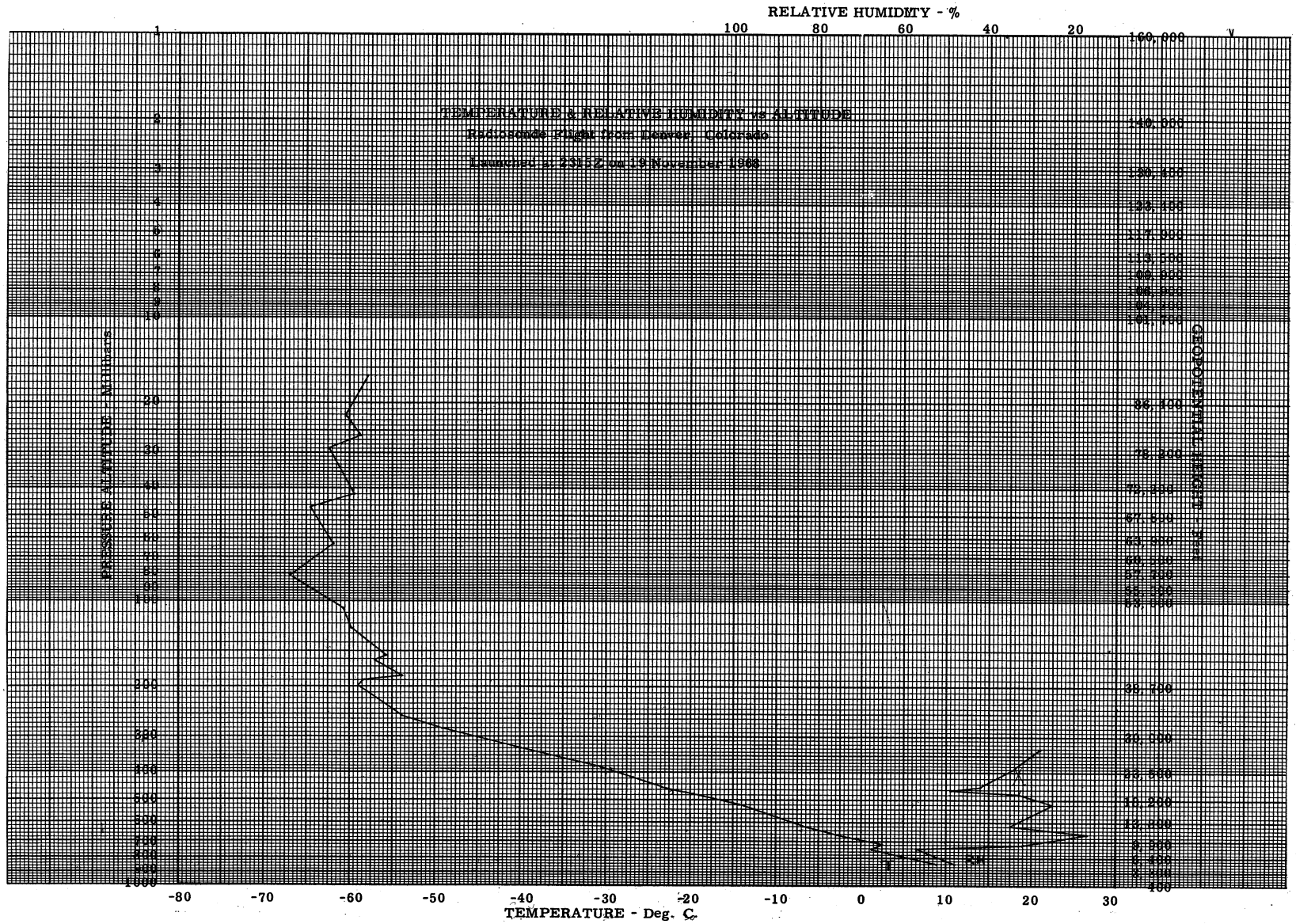

Figure 16. Temperature and Relative Humidity vs. Altitude, Denver, Colorado, 2315 Z, 19 November 1968.

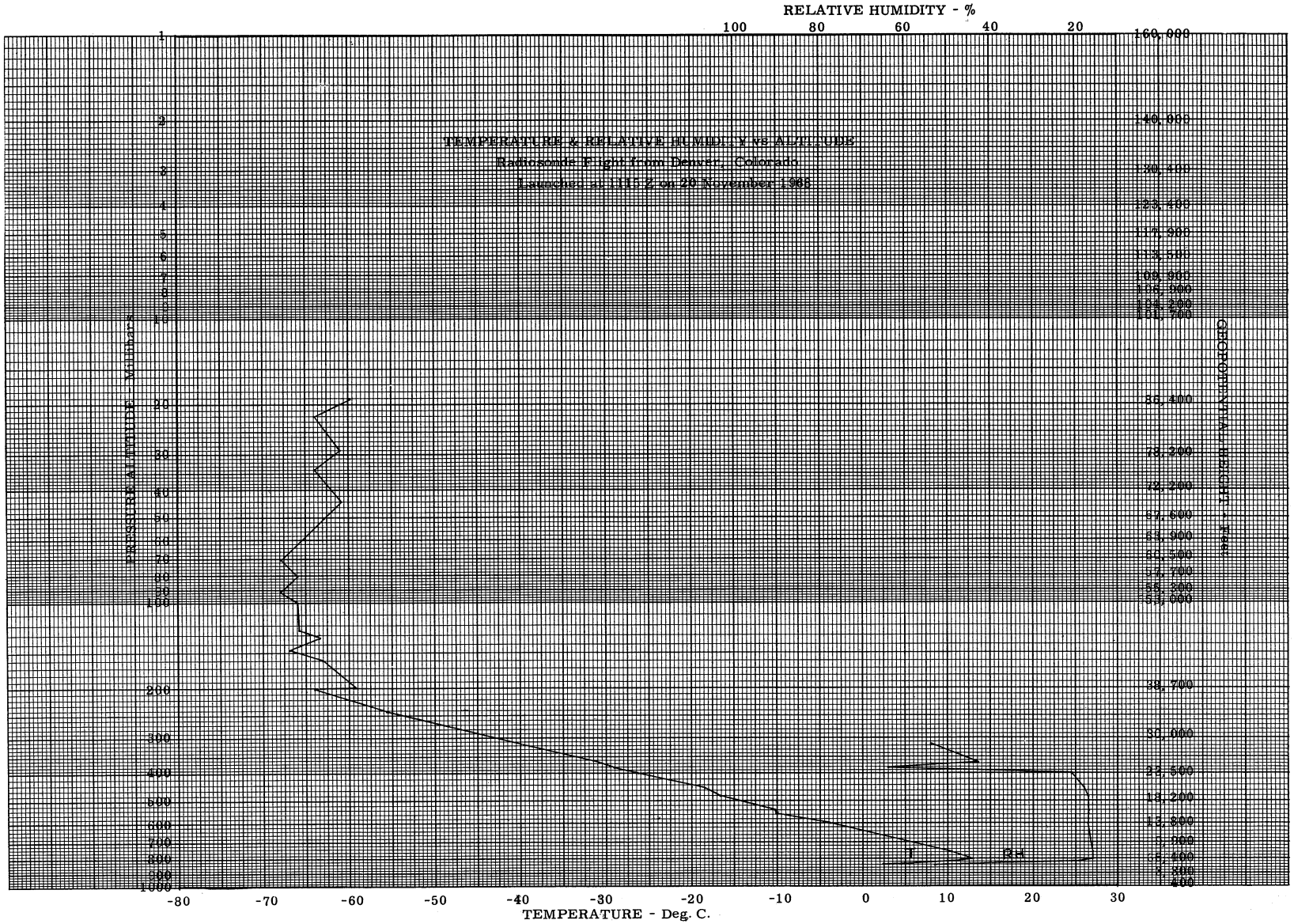

Figure 17. Temperature and Relative Humidity vs. Altitude, Denver, Colorado, 1115Z, 20 November 1968.

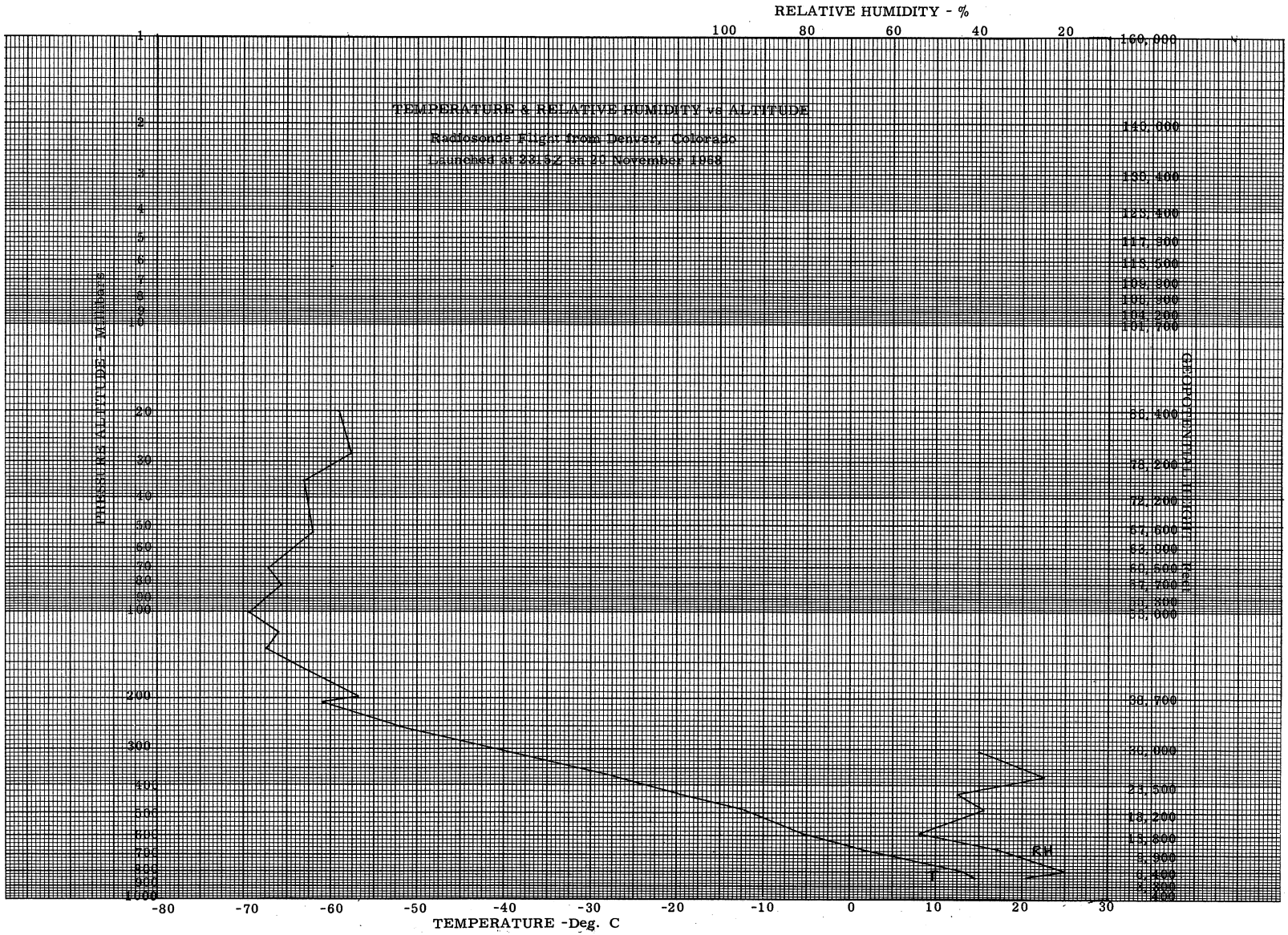

Figure 18. Temperature and Relative Humidity vs. Altitude, Denver, Colorado, 2315Z, 20 November 1968.

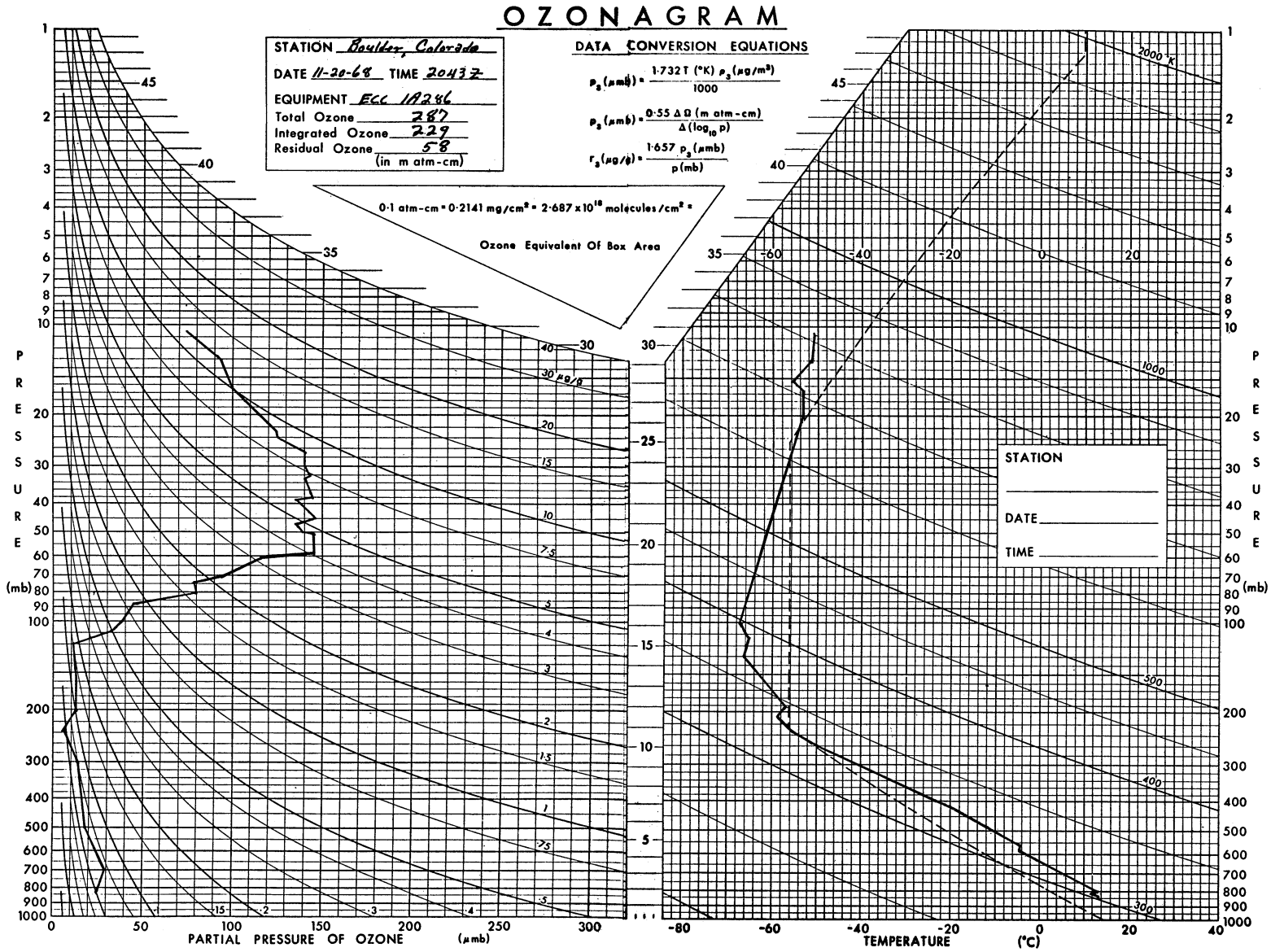

Figure 19. Temperature and Ozone Partial Pressure vs. Altitude, Boulder, Colorado, 2043Z, 20 November 1968.

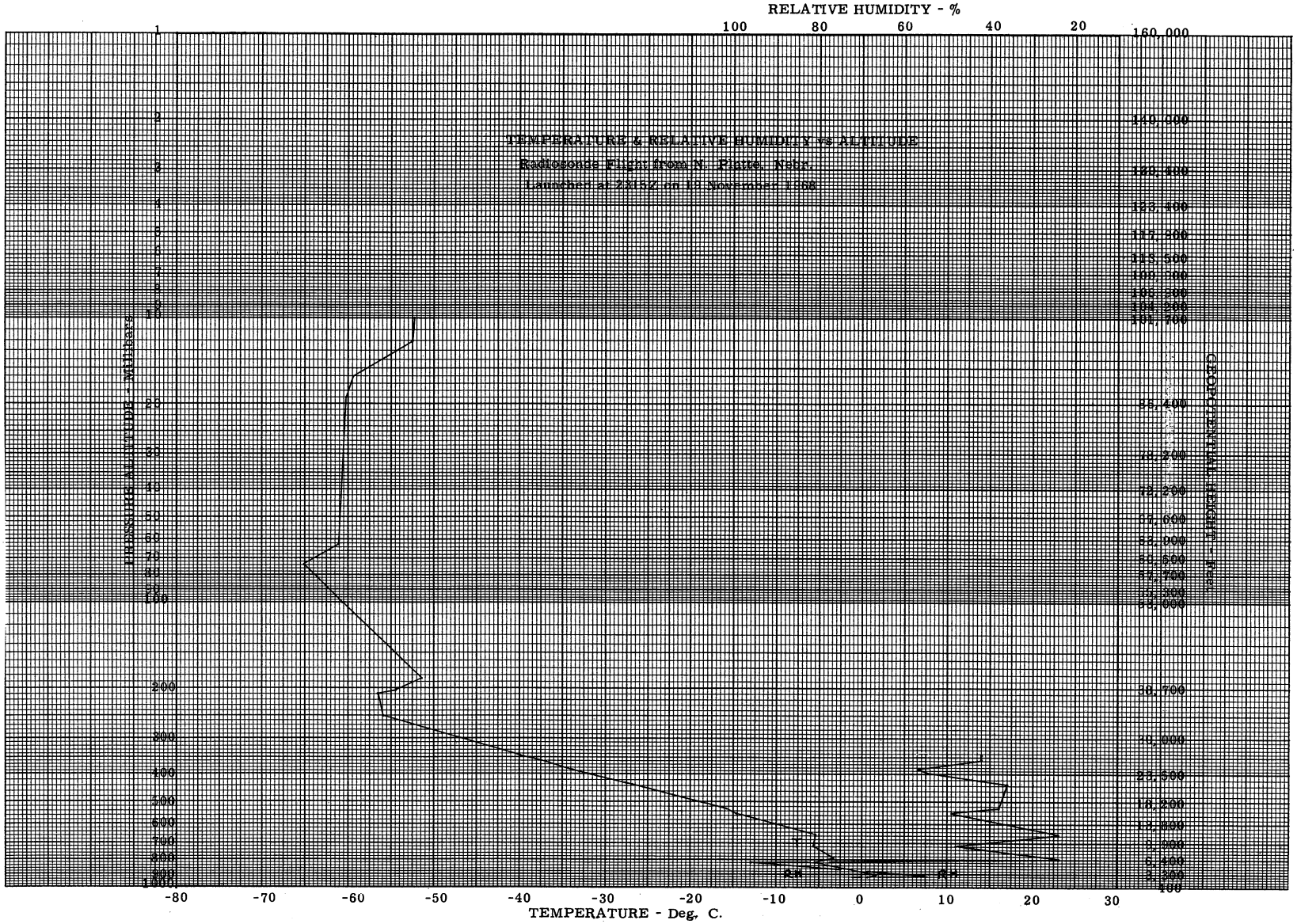

Figure 20. Temperature and Relative Humidity vs. Altitude, N. Platte, Nebraska, 2315Z, 19 November 1968.

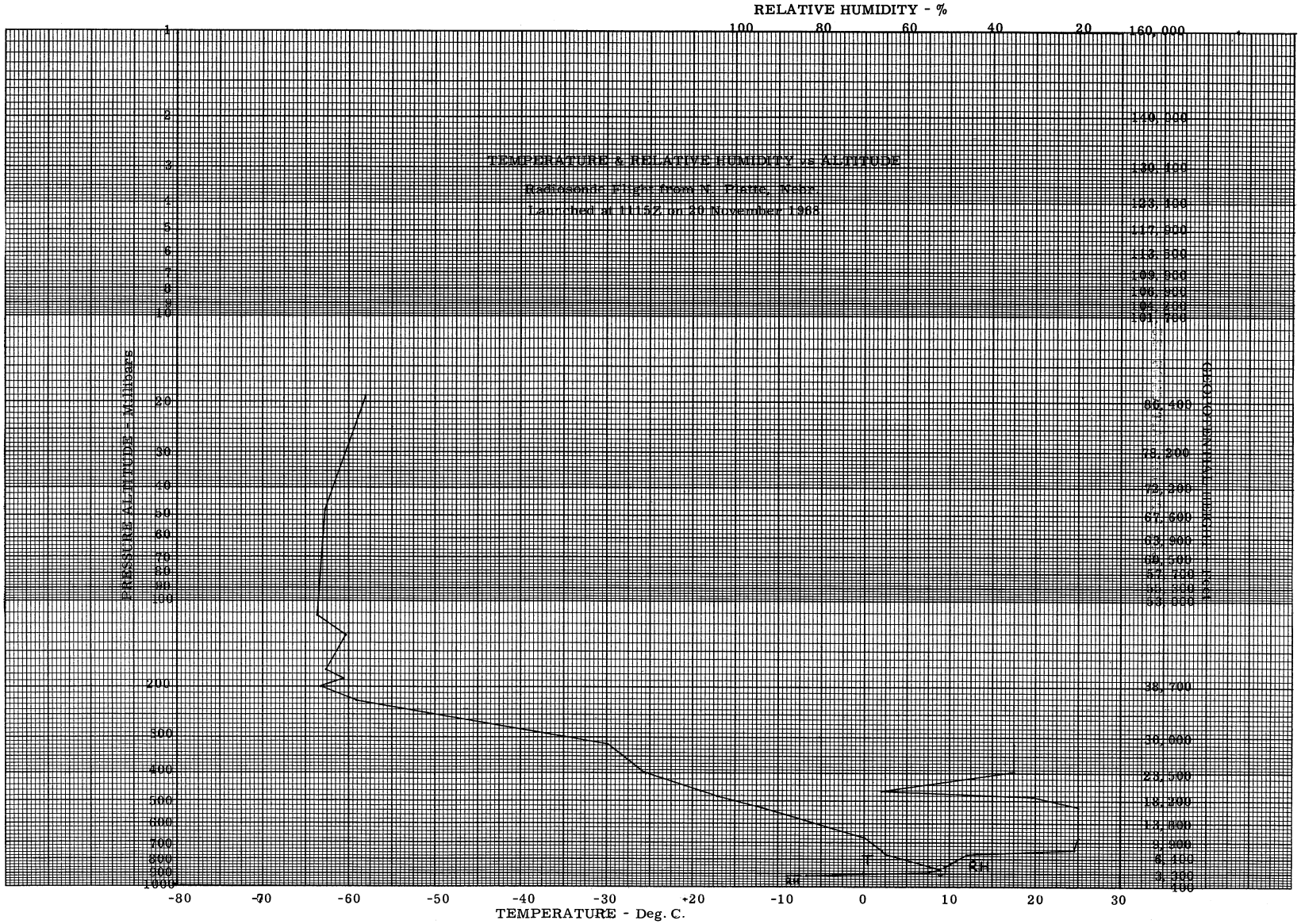

Figure 21. Temperature and Relative Humidity vs. Altitude, N. Platte, Nebraska, 1115Z, 20 November 1968.

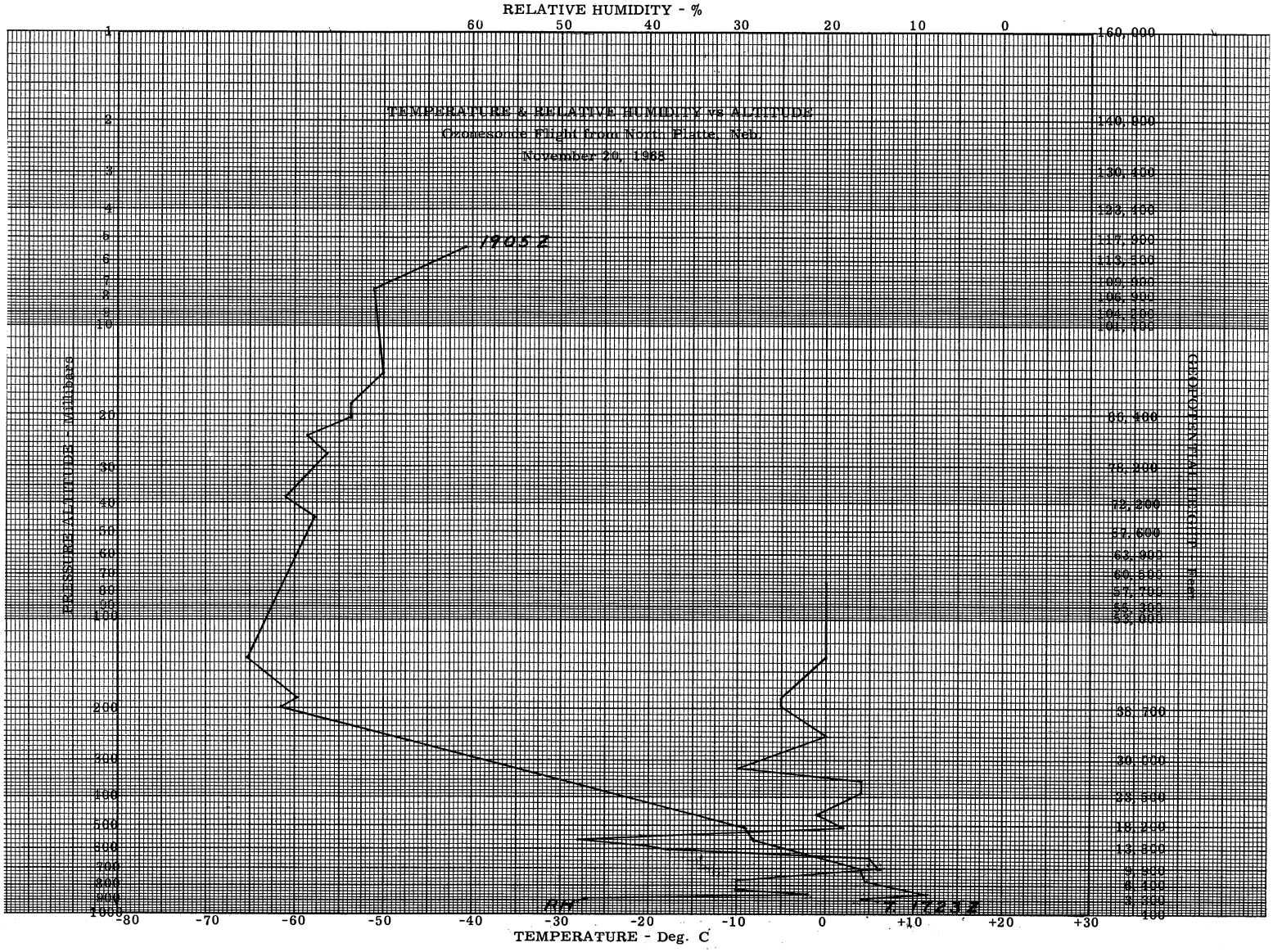

Figure 22. Temperature and Relative Humidity vs. Altitude, N. Platte, Nebraska, 1723Z, 20 November 1968.

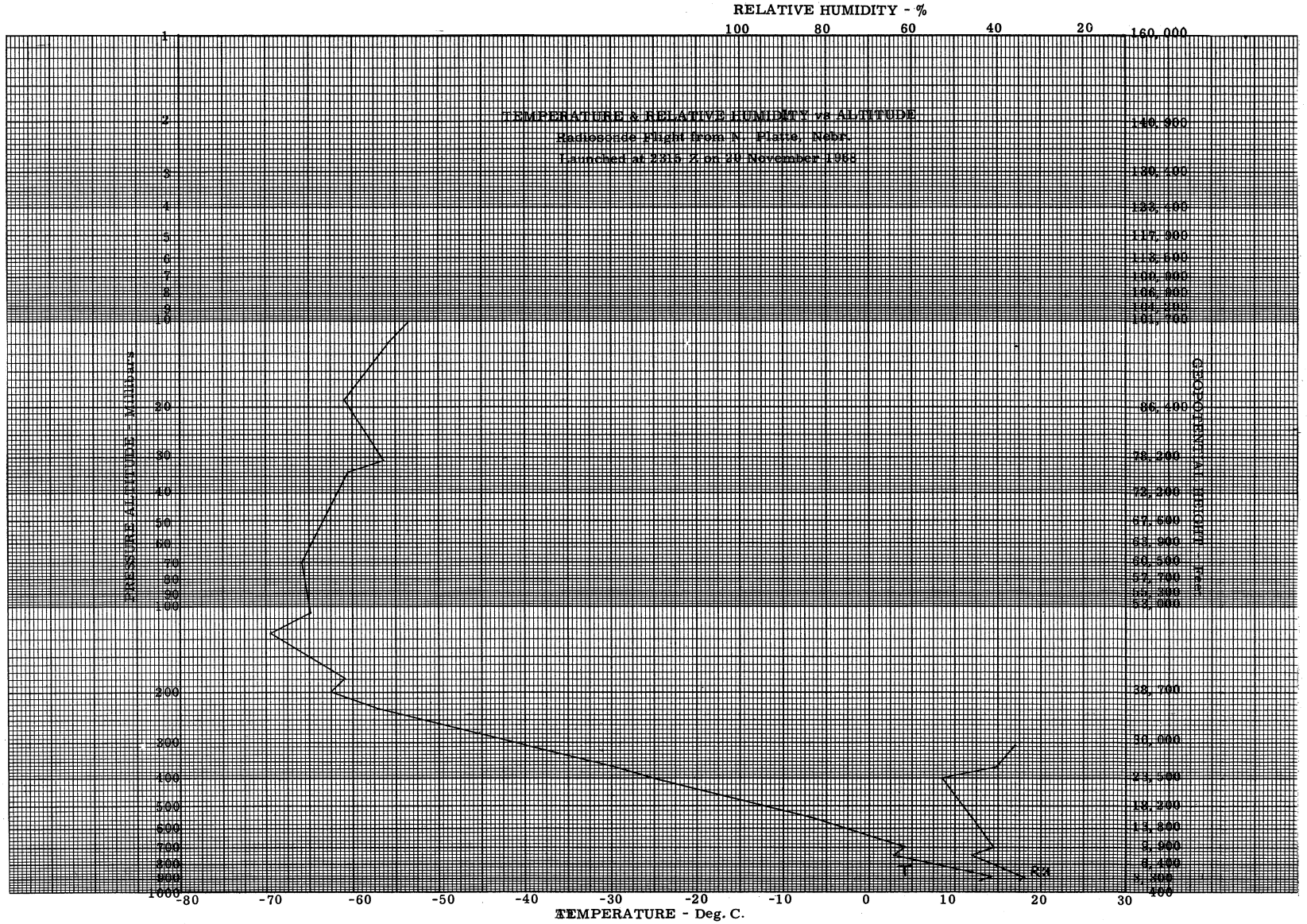

Figure 23. Temperature and Relative Humidity vs. Altitude, N. Platte, Nebraska, 2315Z, 20 November 1968.

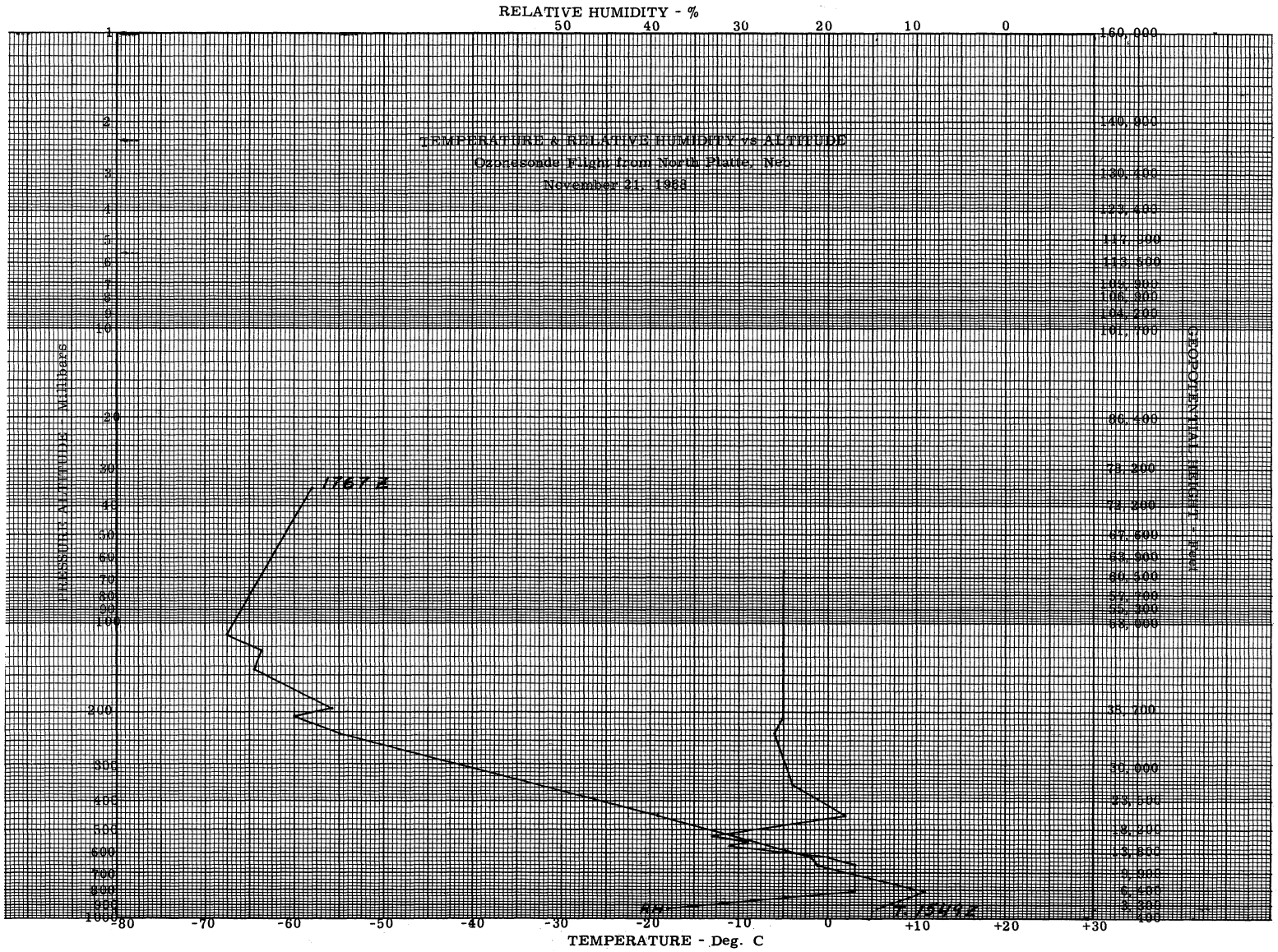

Figure 24. Temperature and Relative Humidity vs. Altitude, N. Platte, Nebraska, 1549Z, 21 November 1968.

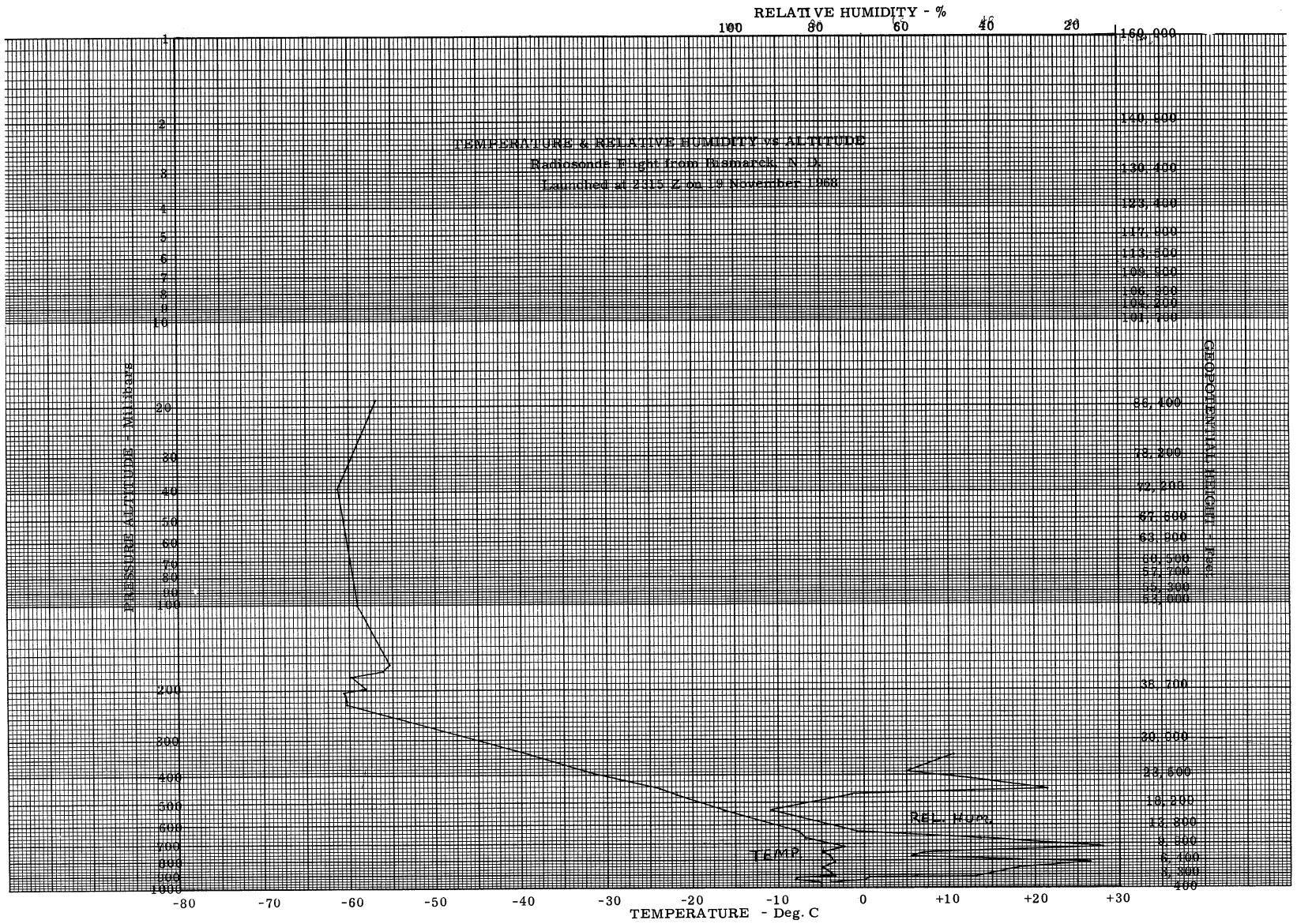

Figure 25. Temperature and Relative Humidity vs. Altitude, Bismarck, North Dakota, 2315Z, 19 November 1968.

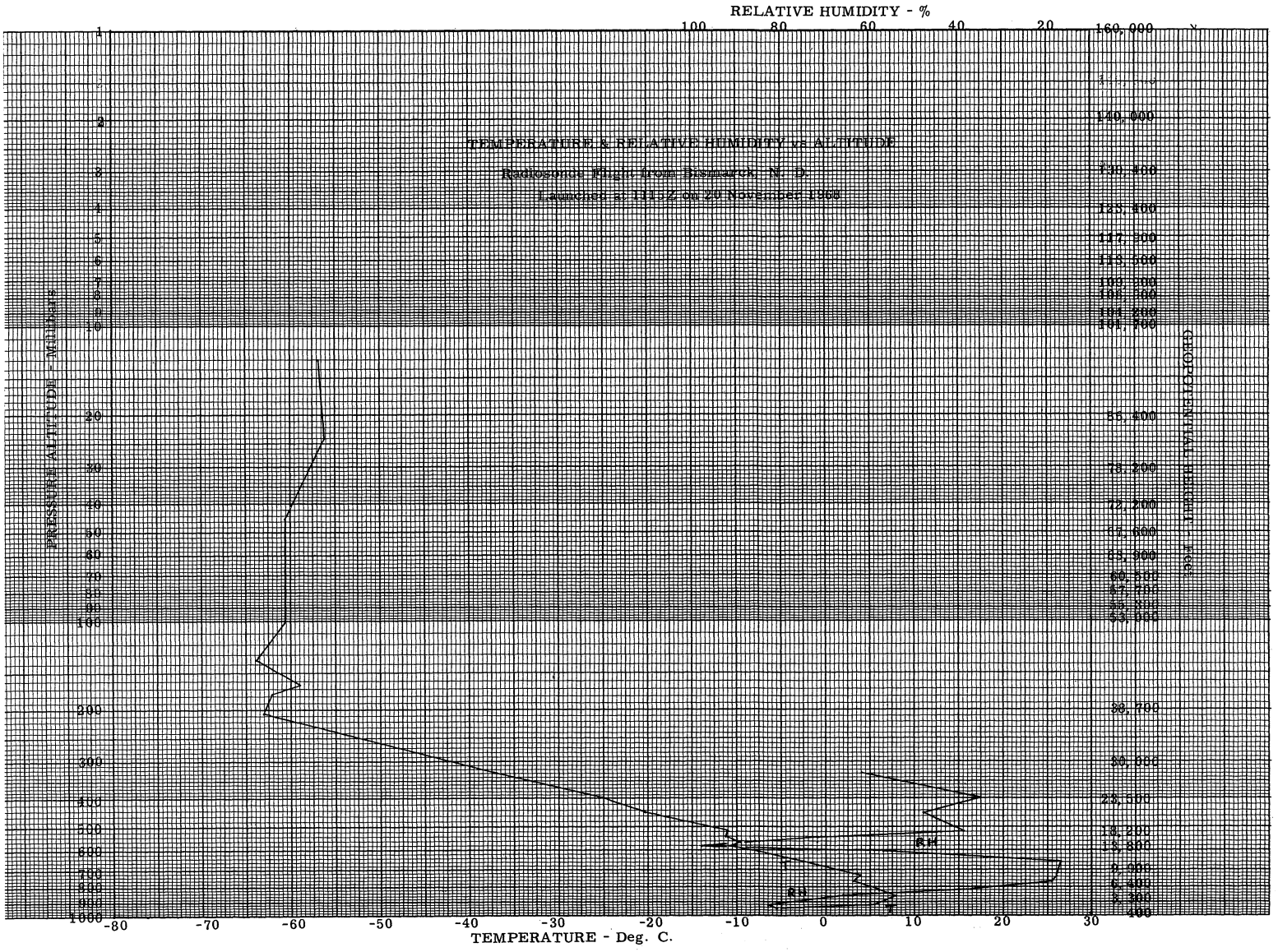

Figure 26. Temperature and Relative Humidity vs. Altitude, Bismarck, North Dakota, 1115Z, 20 November 1968.

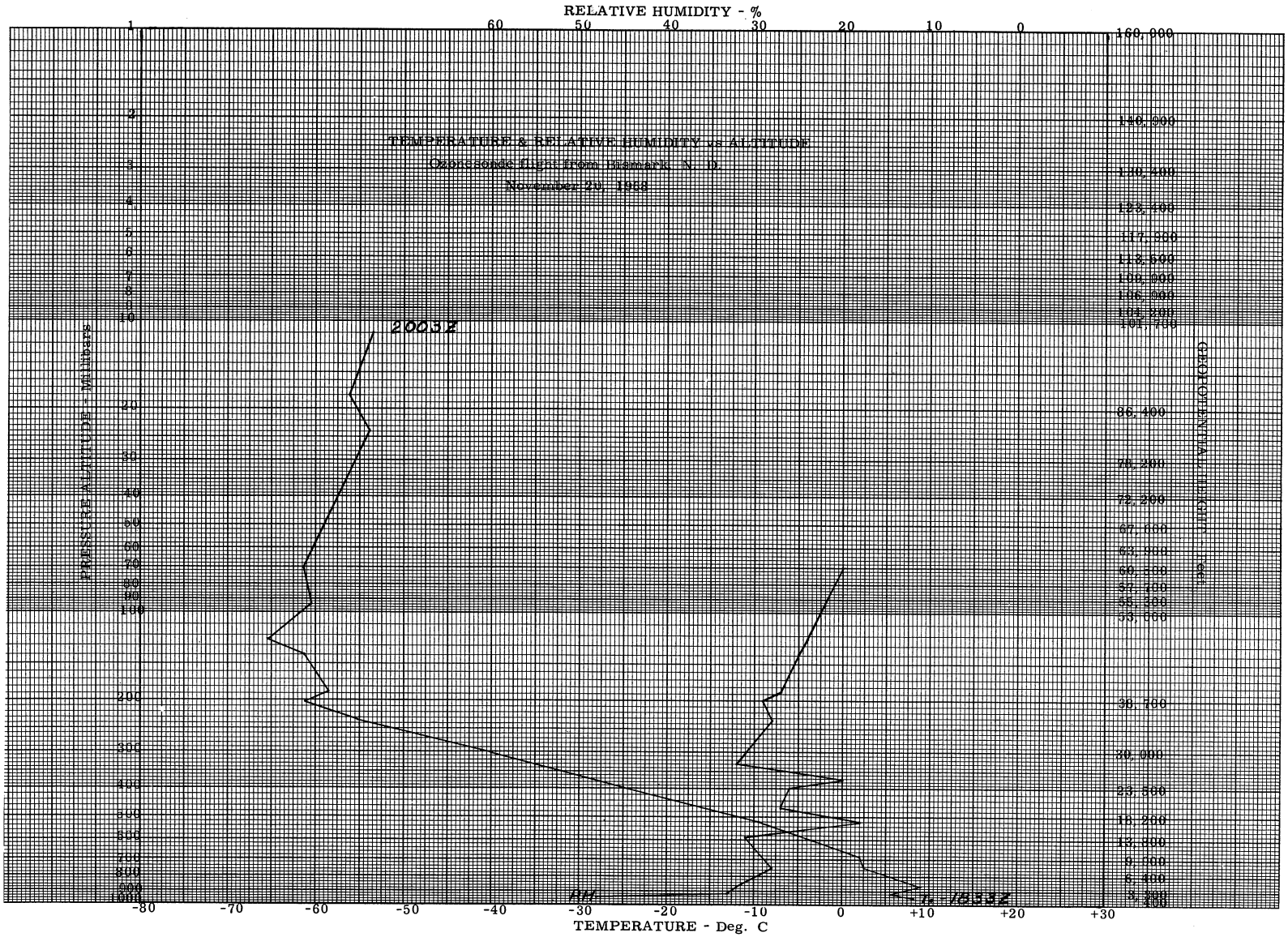

Figure 27. Temperature and Relative Humidity vs. Altitude, Bismarck, North Dakota, 1833Z, 20 November 1968.

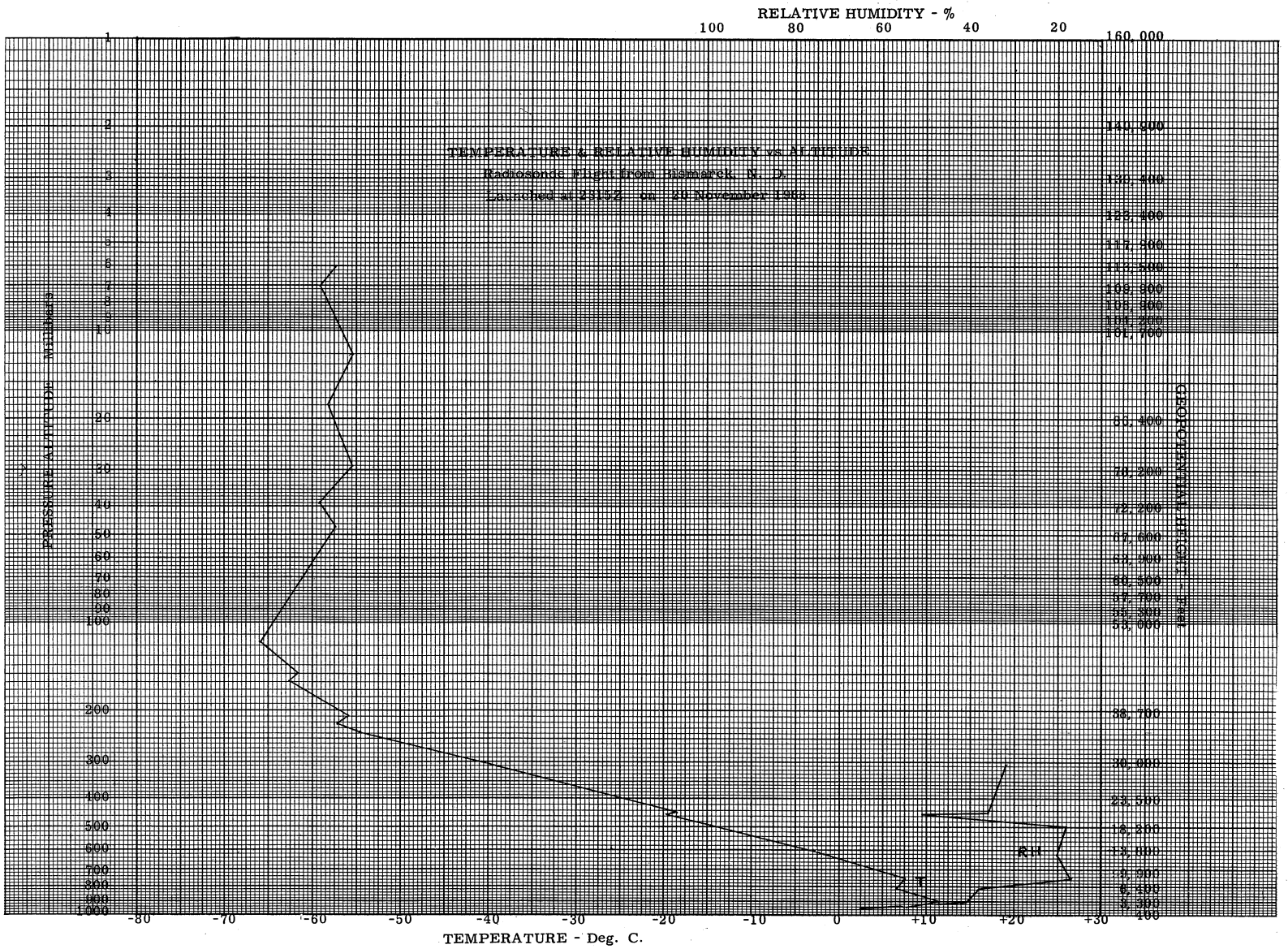

Figure 28. Temperature and Relative Humidity vs. Altitude, B Bismarck, North Dakota, 2315Z, 20 November 1968.

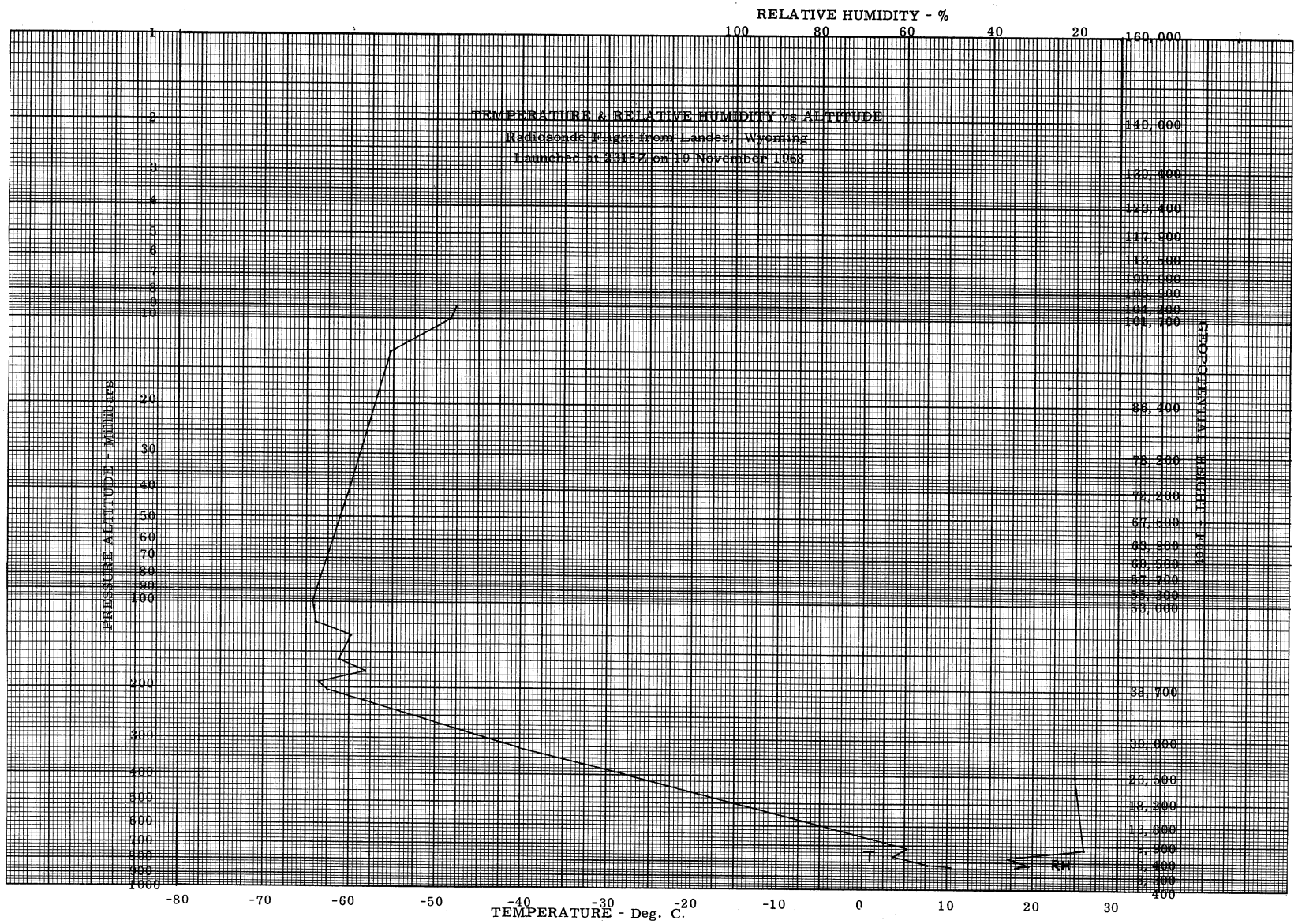

Figure 29. Temperature and Relative Humidity vs. Altitude, Lander, Wyoming, 2315Z, 19 November 1968.

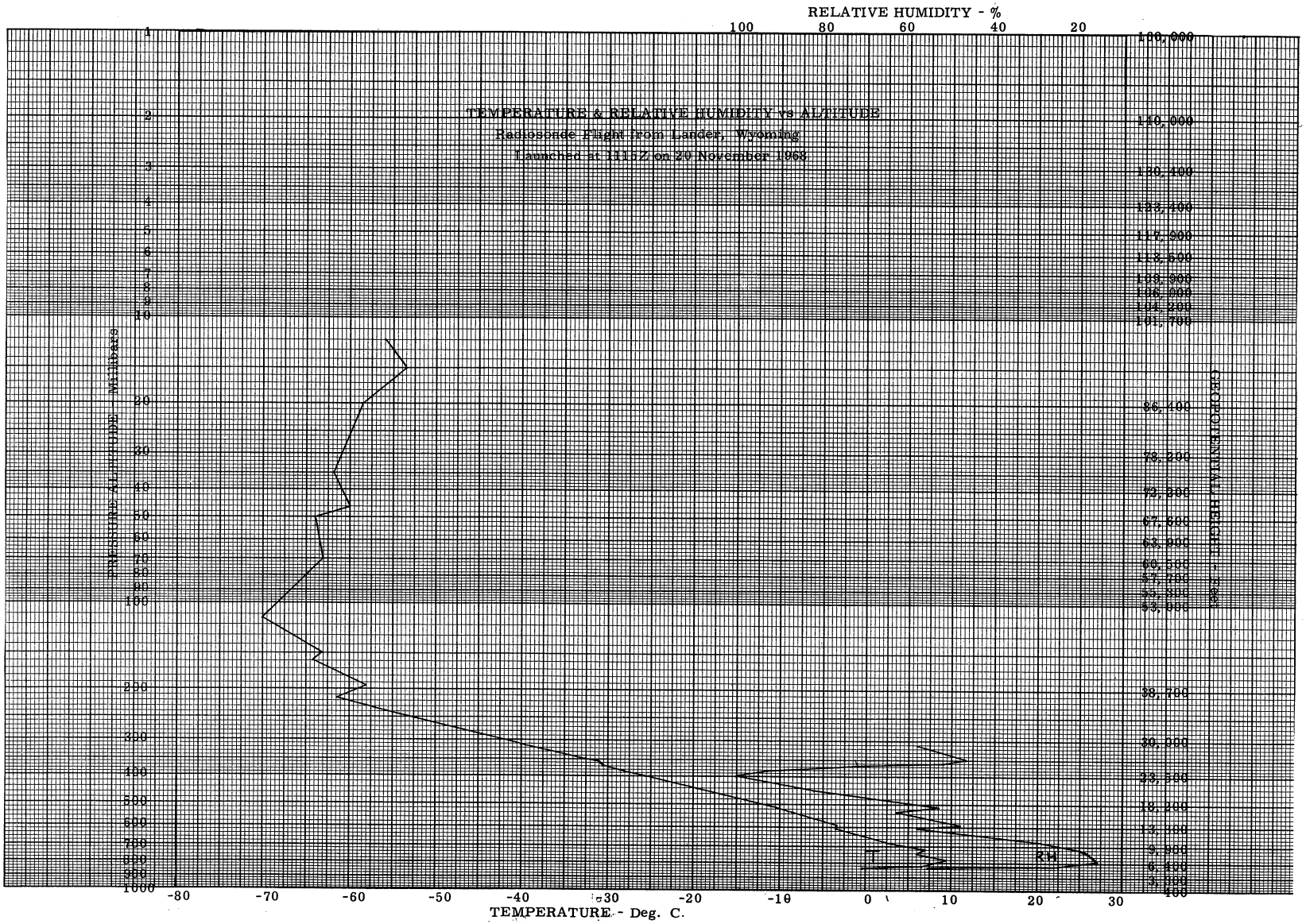

Figure 30. Temperature and Relative Humidity vs. Altitude, Lander, Wyoming, 1115Z, 20 November 1968.

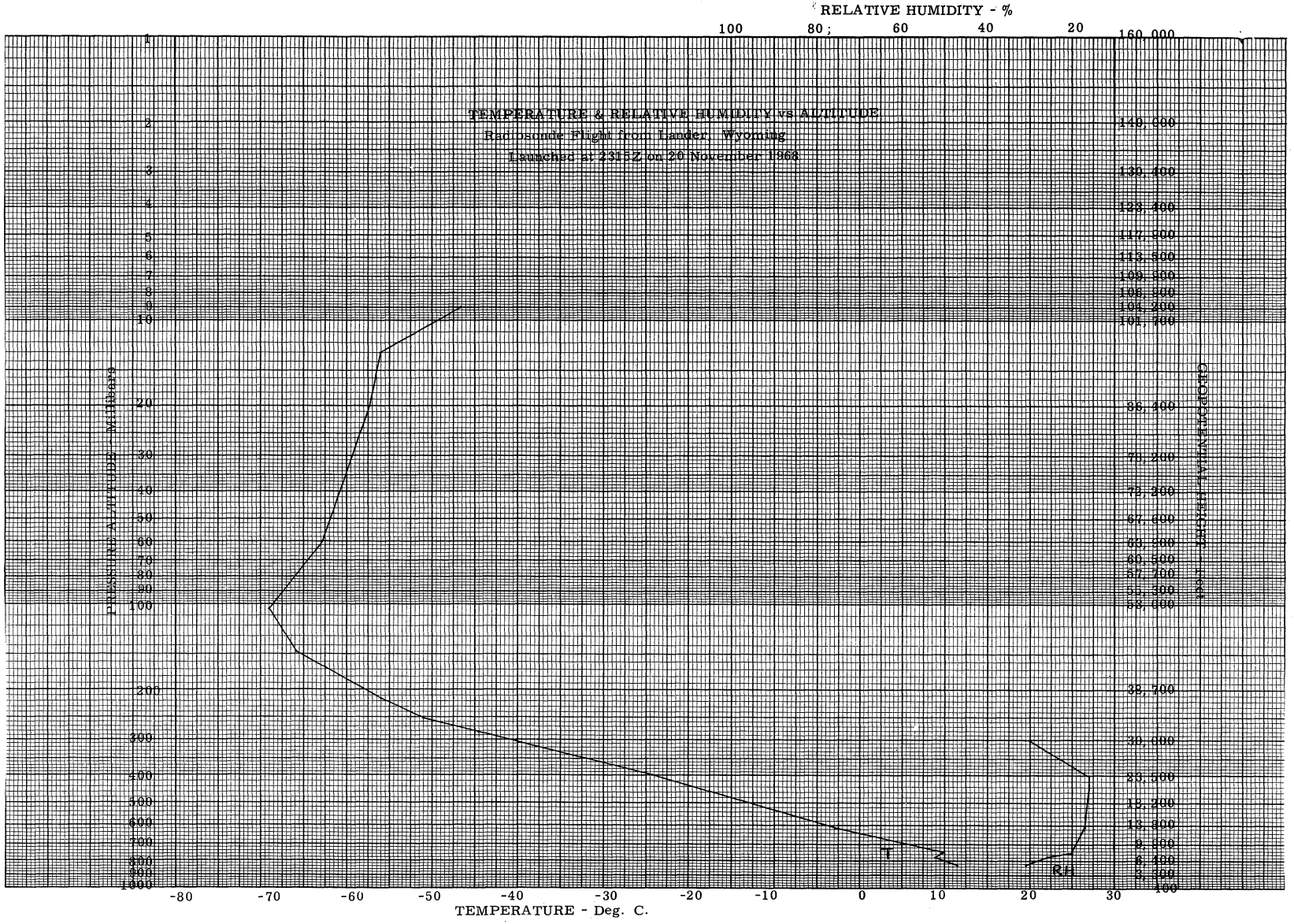

Figure 31. Temperature and Relative Humidity vs. Altitude, Lander, Wyoming, 2315Z, 20 November 1968.

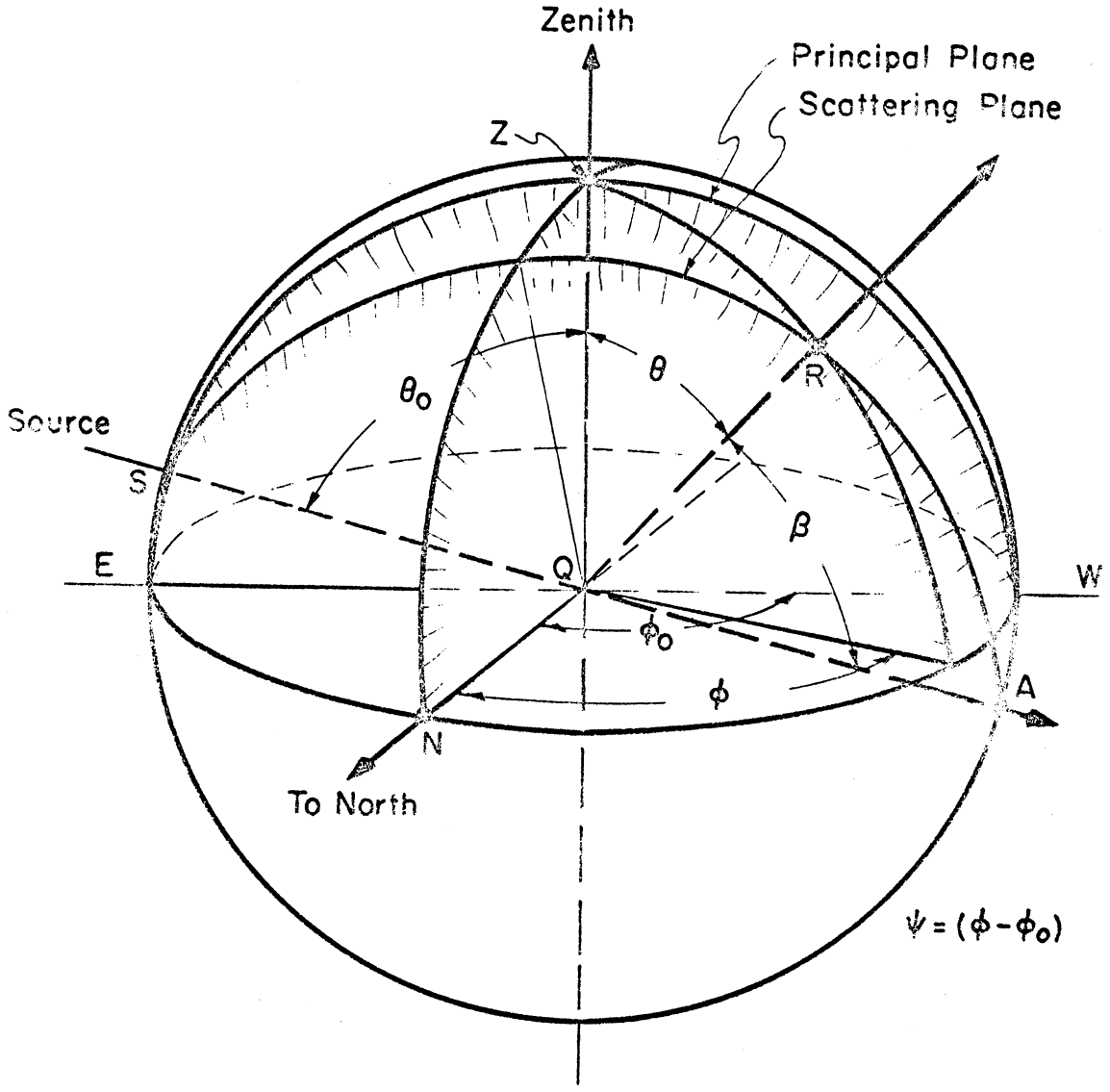

Figure 32. Geometry of Reflection and Scattering

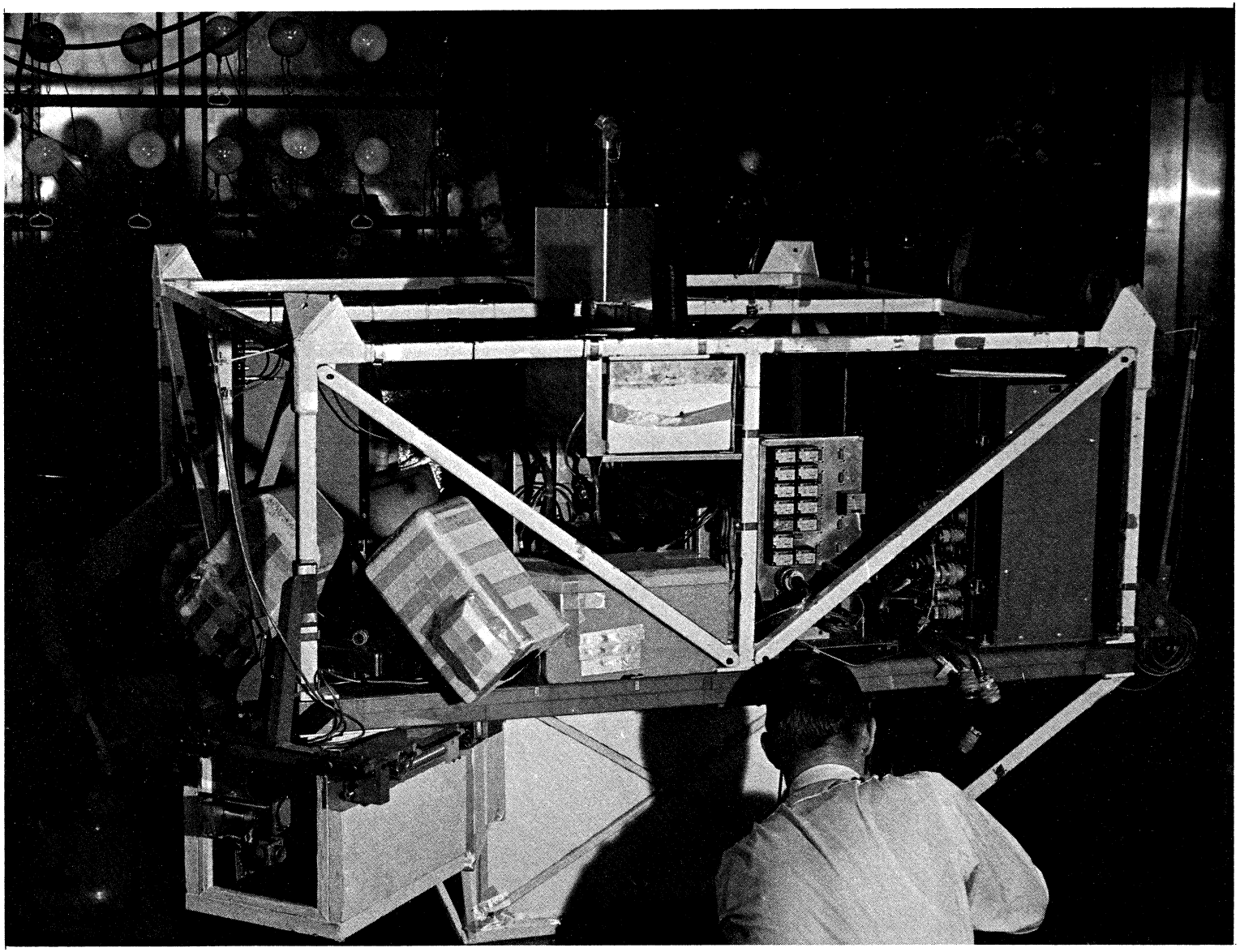

Figure 33. Balloon Gondola, Rotating Photocell at Top.

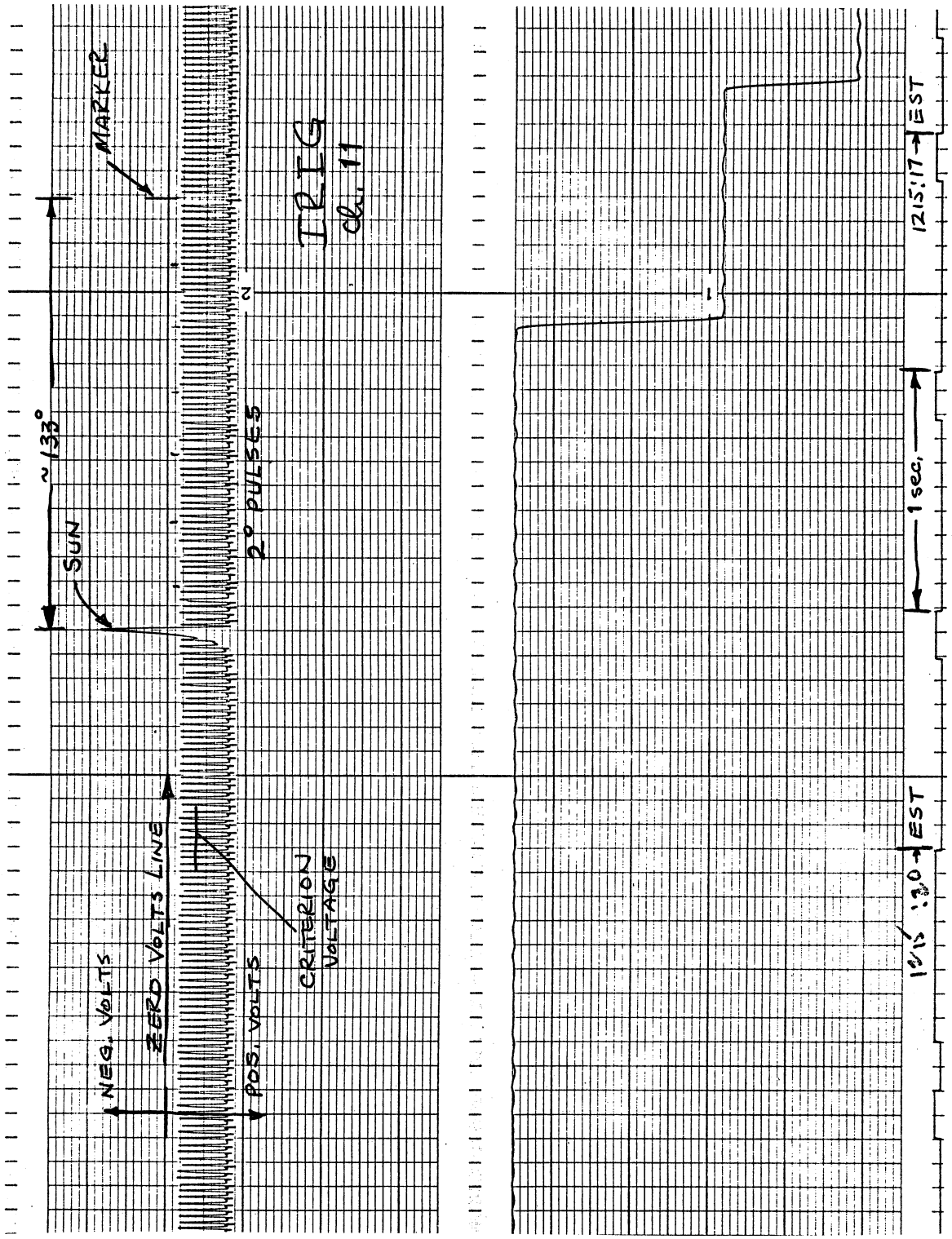

Figure 34. Analog Brush Record of Photocell Data.

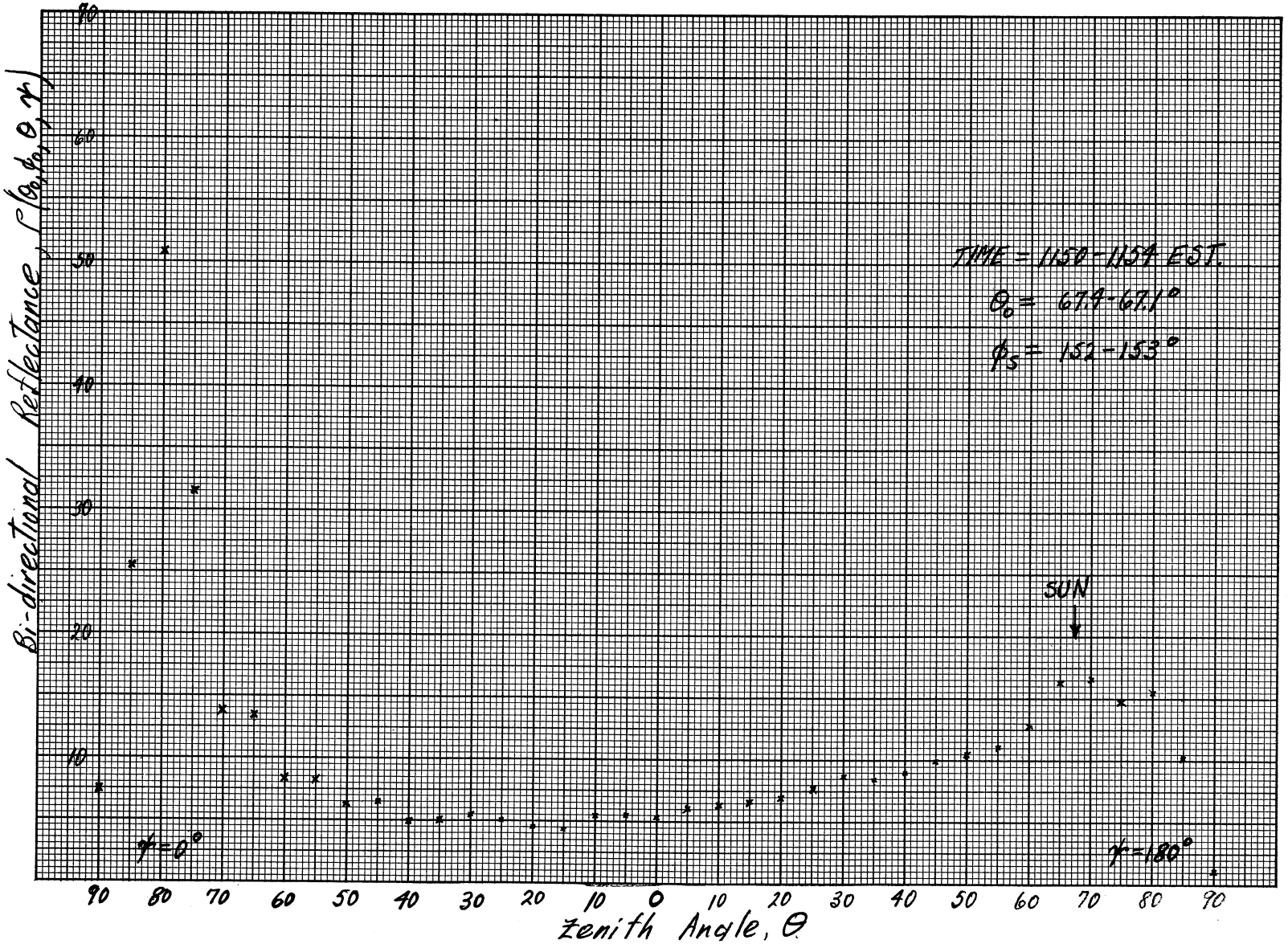

Figure 36. Bi-directional Reflectance in the Principal Plane, 1150-1154 E. S. T.

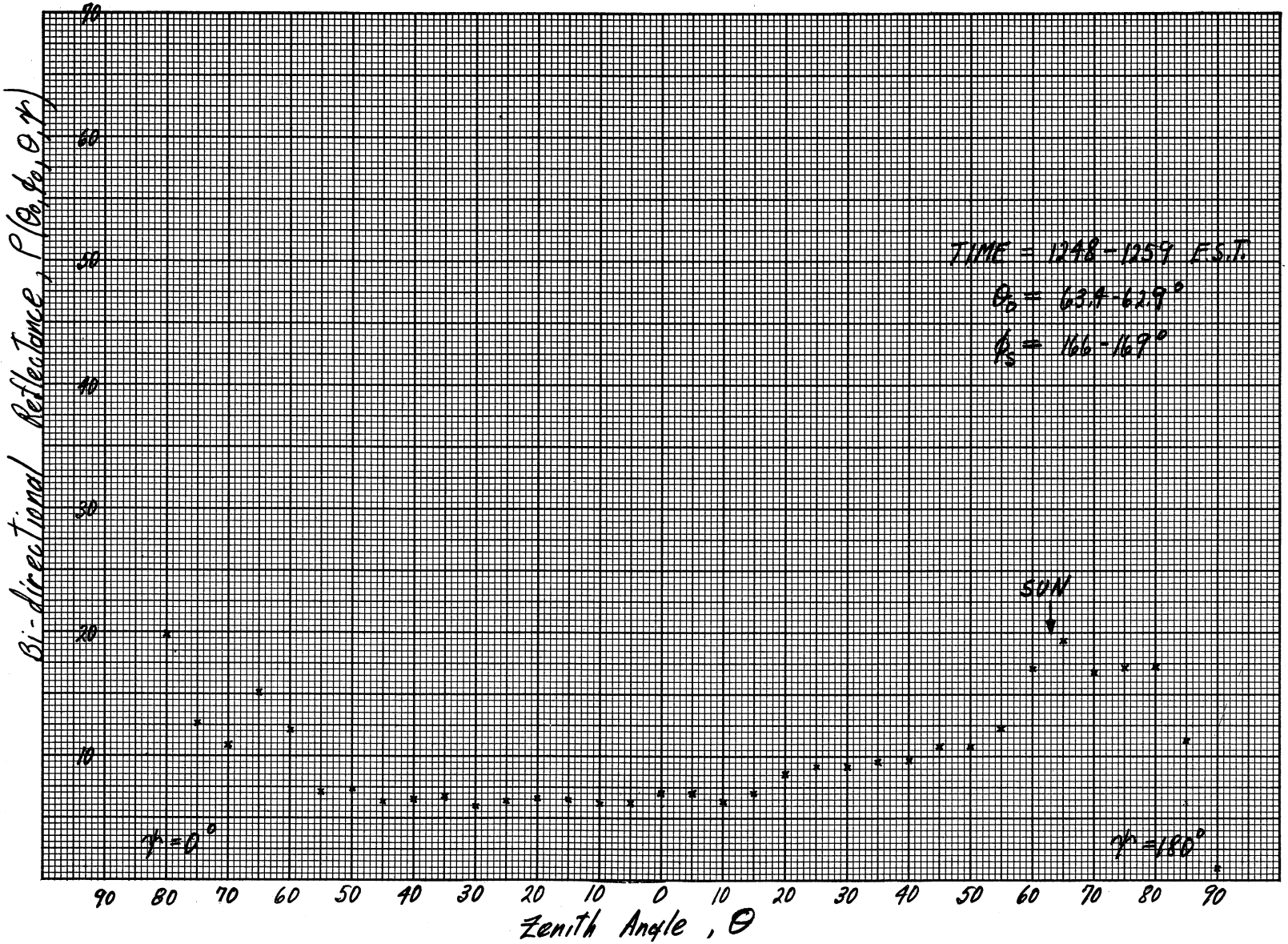

Figure 37. Bi-directional Reflectance in the Principal Plane, 1248-1259 E. S. T.

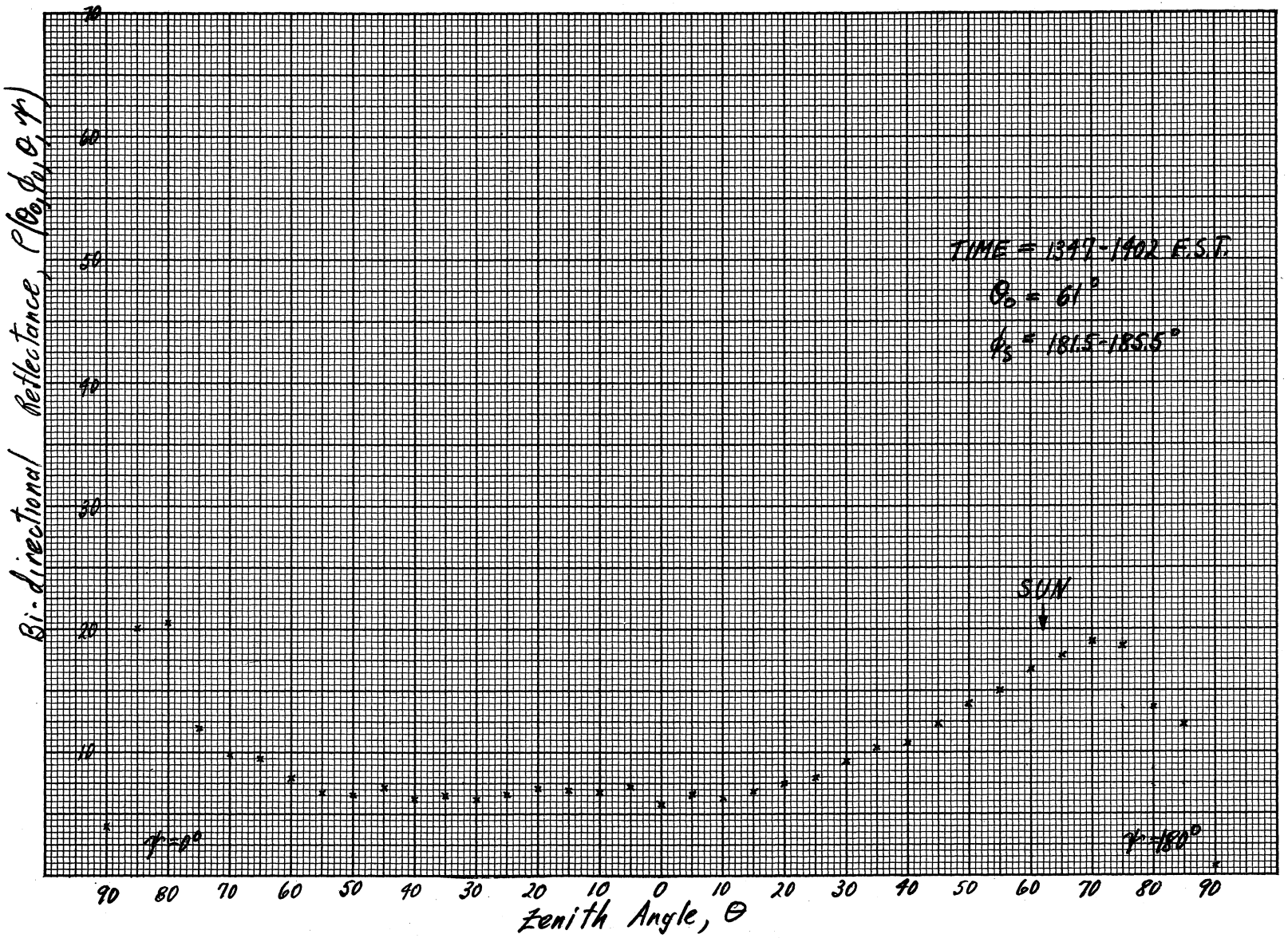

Figure 38. Bi-directional Reflectance in the Principal Plane, 1347-1403 E. S. T.

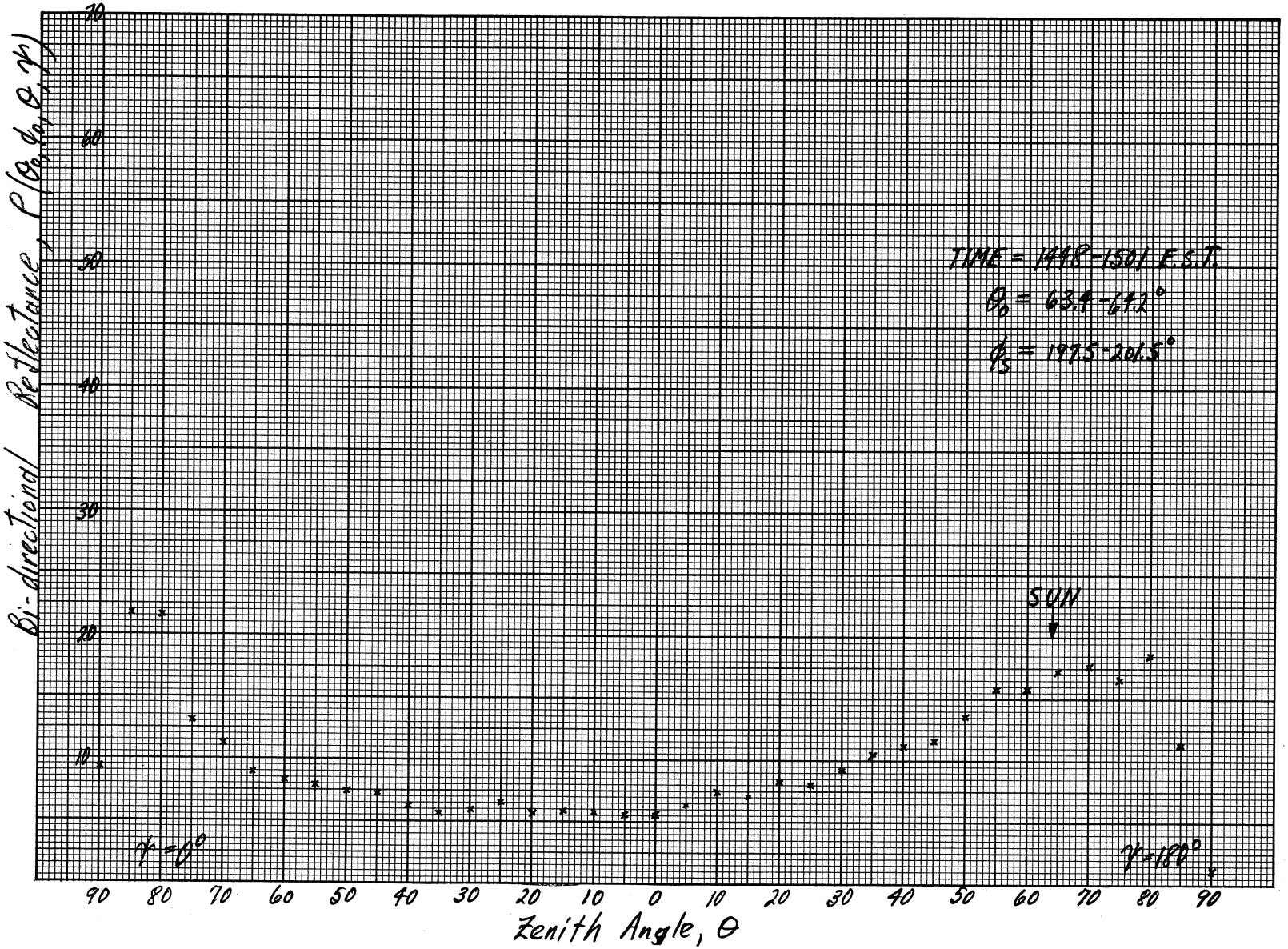

Figure 39. Bi-directional Reflectance in the Principal Plane, 1448-1501 E. S. T.

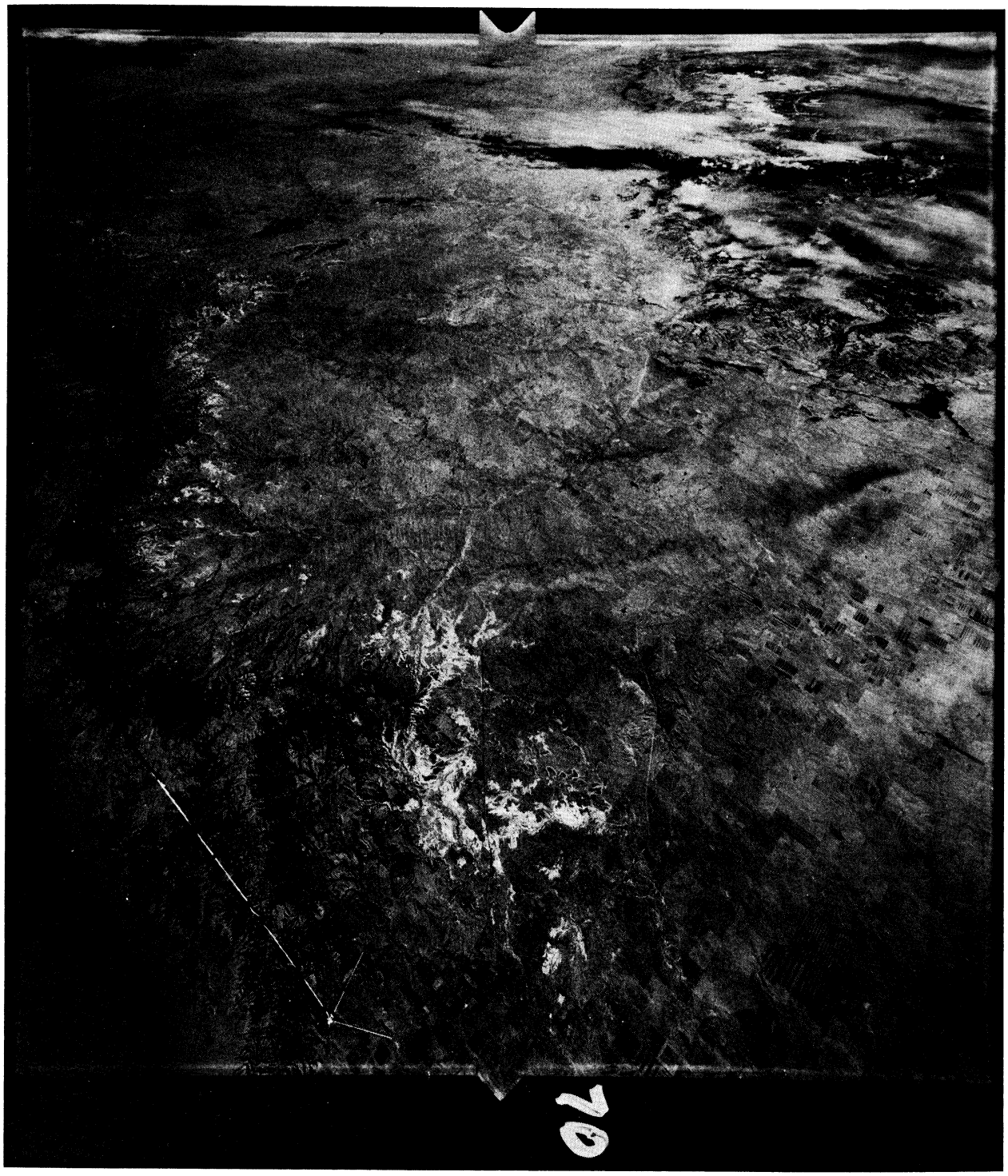

Figure 40. Photo Showing Portion of the Earth for Which Reflectance Data of Figure 36 Applies

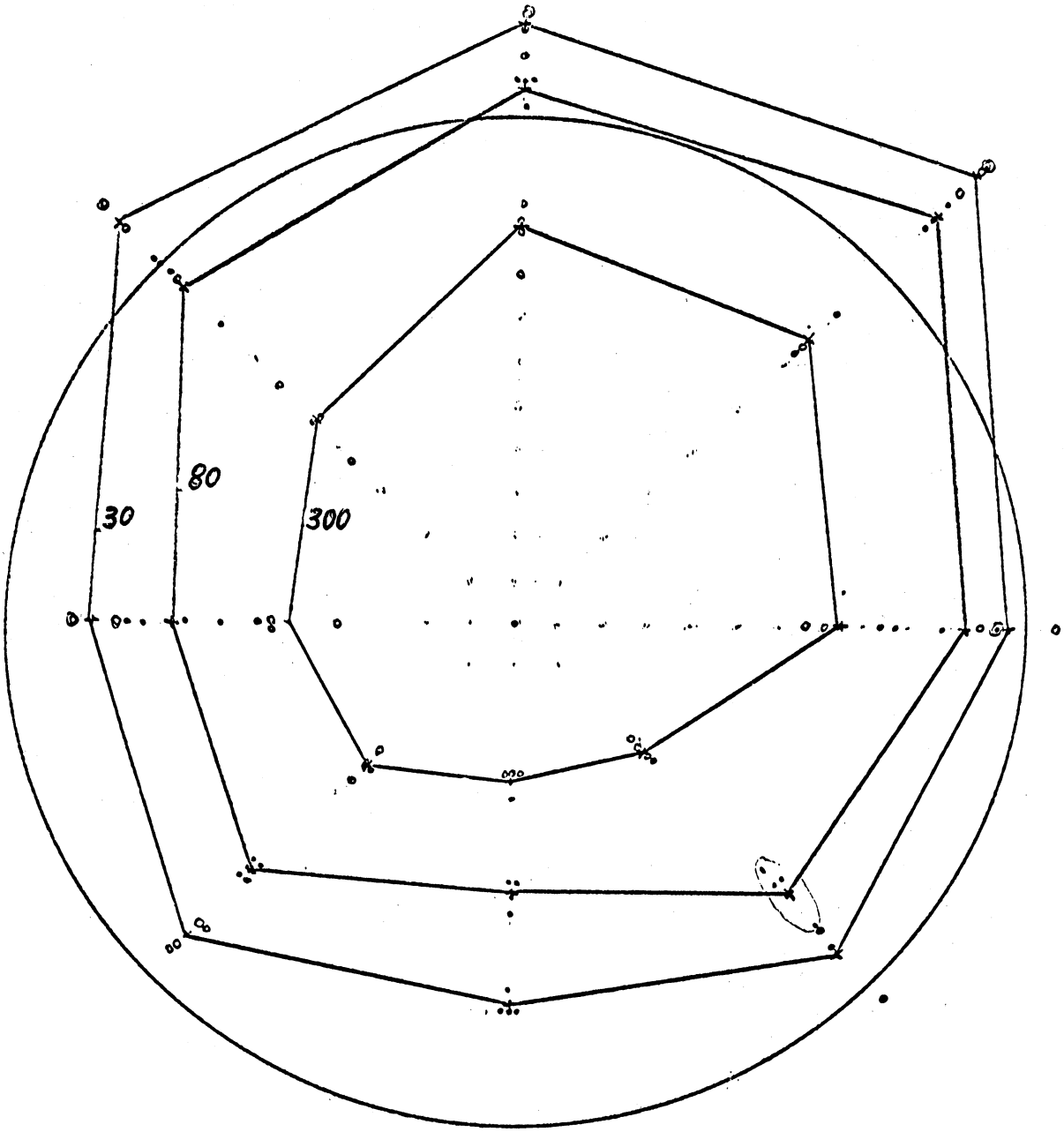

Figure 41. Field of View Contours for IRIS Interferometer